

1 **Model-based analysis of erosion-induced microplastic delivery from arable land to the**  
2 **stream network of a mesoscale catchment**

3 Raphael Rehm<sup>a</sup>, Peter Fiener<sup>a</sup>

4 <sup>a</sup> University of Augsburg, Institute of Geography, *Alter Postweg 118, 86159 Augsburg,*  
5 *Germany*

6 *Correspondance to:* Peter Fiener ([peter.fiener@geo.uni-ausburg.de](mailto:peter.fiener@geo.uni-ausburg.de))

7

## 8 **Abstract**

9       Soils are generally accepted as sinks for microplastic (MP), but at the same time might be a MP source  
10 for inland waters. However, little is known regarding the potential MP delivery from soils to aquatic  
11 systems via surface runoff and erosion. This study provides for the first time an estimate of the extent of  
12 soil erosion-induced MP delivery from an arable-dominated mesoscale catchment (390 km<sup>2</sup>) to its river  
13 network within a typical arable region of Southern Germany. To do this, a soil erosion model was used  
14 and combined with potential particular MP load on arable land from different sources (sewage sludge,  
15 compost, atmospheric deposition and tyre wear) since 1950. The modelling resulted in an annual mean  
16 MP flux into the stream network of 6.33°kg° in 2020, which was dominated by tyre wear (80%). Overall,  
17 0.11–0.17% of the MP applied to arable soils between 1950 and 2020 was transported into the stream  
18 network. In terms of mass, this small proportion was in the same range as the MP inputs from wastewater  
19 treatment plants within the test catchment. More MP (0.5–1% of input between 1950 and 2020) was  
20 deposited in the grassland areas along the stream network, and this could be an additional source of MP  
21 during flood events. Most (5% of the MP applied between 1950 and 2020) of the MP translocated by  
22 tillage and water erosion was buried under the plough layer. Thus, the main part of the MP added to  
23 arable land remained in the topsoil and is available for long-term soil erosion. This can be illustrated  
24 based on a ‘stop MP input in 2020’ scenario, indicating that MP delivery to the stream network until  
25 2100 would only be reduced by 14%. Overall, arable land at risk of soil erosion represents a long-term  
26 MP sink, but also a long-term MP source for inland waters.

27

## 28 **1. Introduction**

29 The global microplastic (MP) contamination of different environmental compartments is currently the  
30 focus of different research fields (Nasseri and Azizi, 2022; Tian et al., 2022; Zhang et al., 2022). Among  
31 these, MP in soils have increasingly received scientific attention (Chia et al., 2021; Sajjad et al., 2022;  
32 Zhou et al., 2020). Microplastic is mostly referred as plastic particles or fibres in a size range of 1 to  
33 5000  $\mu\text{m}$ , originating from the breakdown of larger plastic items or manufacturing at this scale for  
34 various purposes (Frias and Nash, 2019; Kim et al., 2021). Many MP sources have been identified for  
35 soil systems. Next to tyre wear (TW), stated as the main source (Knight et al., 2020a; Sommer et al.,  
36 2018), littering (Scheurer and Bigalke, 2018) and atmospheric deposition (Brahney et al., 2020) also  
37 serve as MP input pathways. Arable soils in particular often experience additional MP inputs associated  
38 to agricultural soil management (Brandes, 2020). Mulch films (Ng et al., 2020), the use of compost and  
39 sewage sludge as organic fertilizers (Braun et al., 2021; Liu et al., 2014; Zhang et al., 2020), irrigation  
40 with contaminated (waste) water (Pérez-Reverón et al., 2022), as well as MP associated with coated  
41 fertilizer and seeds (Accinelli et al., 2021; Lian et al., 2021), have proven to be the main input paths. MP  
42 enters the soil system mostly via the surface and is mixed into the soil column via bioturbation (Heinze  
43 et al., 2022; Li et al., 2021) and, in the case of small particles, via infiltration (Li et al., 2021). In arable  
44 land, it is actively mixed into the plough layer via tillage operations (Weber et al., 2022; Zhao et al.,  
45 2022; Zubris and Richards, 2005). Depending on the tillage technique, the MP is worked into the soil at  
46 different depths and is more or less homogenized after multiple processing (Fiener et al., 2018; Weber  
47 et al., 2022). Moreover, tillage potentially leads to mechanical fragmentation of macroplastic but also  
48 reduces photochemical decomposition at the soil surface and reduces MP transport via water and wind  
49 (Colin et al., 1981; Corcoran, 2022; Feuilleley et al., 2005).

50 Despite the known pathways into the soil, knowledge of the fate of MP particles once they enter the  
51 soil system is limited (Guo et al., 2020; Hurley and Nizzetto, 2018; Tian et al., 2022). However, the

52 question arises as to whether the terrestrial MP sink releases relevant amounts of MP for water bodies  
53 via water erosion. If so, the soils, as an MP sink, could represent an important MP source for water  
54 bodies. Besides very slow, not very well determined processes of plastic fragmentation (Corcoran, 2022),  
55 there is also only a small number of studies analysing vertical MP transport due to bioturbation (Heinze  
56 et al., 2022; Li et al., 2021) and leaching (Chia et al., 2021; Viaroli et al., 2022) within the soil column,  
57 or lateral losses to other ecosystems via erosion processes (Borthakur et al., 2022; Bullard et al., 2021;  
58 Rehm et al., 2021).

59 The potential lateral transport via (water) erosion processes might be analysed using existing  
60 modelling techniques. Such approaches face two major challenges: modelling approaches are required  
61 which allow the cumulative loss of MP to adjacent ecosystems to be determined while taking spatial  
62 differences in MP contamination and site-specific erosion into account. Moreover, the long-term change  
63 in MP concentrations in the plough layer should be considered, following mixing with subsoil at  
64 erosional sites or burial of MP below the plough layer at depositional sites.

65 In general, there are different water erosion modelling approaches available, ranging from physically-  
66 oriented models (MCST, Fiener et al., 2008; e.g. EROSION3D, Schmidt et al., 1999), which might be  
67 suitable for dealing with the specific particle size and density of MP during transport in the case of  
68 individual erosion events, to conceptual approaches e.g. WaTEM/SEDEM, (Van Oost et al., 2000; Van  
69 Rompaey et al., 2001), which are able to consider long-term cumulative MP soil contamination and the  
70 associated long-term soil and MP erosion, transport and deposition. In general, models of the first type  
71 are very parameter and input data intensive and are mostly applied in small catchments, while the second  
72 type of model needs less detailed data and is often used for mesoscale catchments (Nunes et al., 2018).  
73 Following the requirements outlined above, conceptual, long-term approaches that account for spatial  
74 variability in MP soil contamination and erosion processes seemed to be more appropriate than process-  
75 oriented models to simulate the magnitude of erosion-induced MP delivery to the stream network of

76 mesoscale catchments. As MP loss below the plough layer might be also important in reducing topsoil  
77 MP contamination, such a model approach should not only simulate water erosion, but also tillage  
78 erosion processes leading to a reduction of the MP concentration at erosional sites and MP burial below  
79 the plough layer at depositional sites. One of the few models simulating long-term water and tillage  
80 erosion in a spatial context that updates the soil properties within the soil profile is the SPEROS-C model  
81 (Fiener et al., 2015; Van Oost et al., 2005b). The water and tillage erosion components of the model,  
82 originating from the WaTEM/SEDEM model (Van Oost et al., 2000; Van Rompaey et al., 2001), were  
83 tested in several micro- and mesoscale catchments (Krasa et al., 2005; Verstraeten and Prosser, 2008).

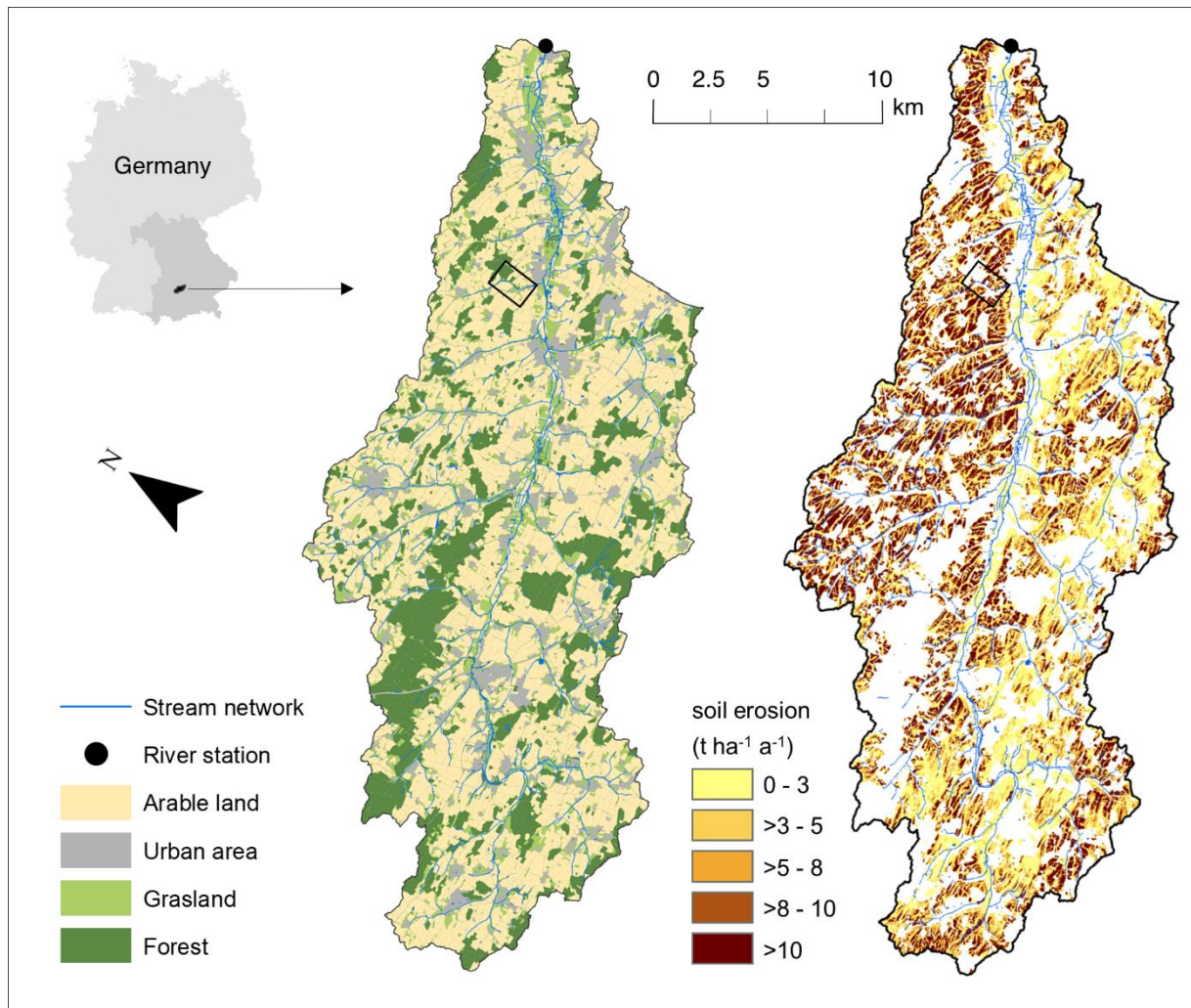
84 The general objective of this study is to investigate MP transport from arable land to the stream  
85 network in an example mesoscale (390 km<sup>2</sup>) arable catchment in Southern Germany. Therefore, the  
86 model SPEROS-C was adjusted to study the importance of water and tillage erosion processes for  
87 particular MP transport. Specifically, this study focuses on the following areas: (i) quantifying the  
88 importance of the water erosion pathway for MP input to the stream network in an example mesoscale  
89 catchment, while taking into account the large uncertainties, particularly in estimates of MP input to soil;  
90 (ii) determining the importance of different erosion processes in changing the MP concentration in the  
91 plough layer and burying MP below the plough layer, and (iii) using scenarios to determine future  
92 pathways of diffuse MP delivery into the stream network.

## 93 **2. Methods**

### 94 *2.1. Test catchment*

95 The catchment was chosen for two main reasons: (i) it represents an intensively used arable landscape  
96 in Southern Germany with hilly terrain and highly productive, loess-burden soils, and (ii) the Bavarian  
97 States Office for Environment has monitored discharge and sediment delivery at the outlet since 1968,  
98 which allows the erosion component of the model to be tested. The mesoscale Glonn catchment

99 (48°22'N, 11°24'E) covers 390 km<sup>2</sup> and its altitude ranges from 578 m in its south-west to 447 m a.s.l.  
100 at its outlet in the north-east (Fig. 1). Mean annual temperature and mean precipitation of the region are  
101 7.5°C and 876 mm respectively, with the most intense rainfall events associated with convective rainfall  
102 in summer. The hilly landscape ( $4.7\pm 3.7^\circ$  main slope) is characterized by loamy Cambisols (WRB, 2015)  
103 on the elevated terrain and loamy Gleysols (WRB, 2015) in the valleys. Land cover in this area is  
104 dominated by arable land (54%), followed by forest (21%), grassland (14%) and settlements (11%) (Fig.  
105 1). The main crops are arranged in a corn-grain rotation. Due to the rolling topography and the erosion-  
106 prone soils, a potential long-term mean soil erosion of 5.9 t ha<sup>-1</sup> a<sup>-1</sup> (based on the German version of the  
107 Universal Soil Loss Equation ABAG) could be calculated for arable land within the catchment (Lfl,  
108 2023) with potential erosion rates up to 10 t ha<sup>-1</sup> a<sup>-1</sup> (Fig. 1).



109  
 110 **Figure 1: The Glonn catchment (390 km<sup>2</sup>) representing a typical intensively used arable landscape**  
 111 **in Southern Germany. The left and right maps show the land use and the soil erosion within the**  
 112 **catchment (with a potential long-term mean soil erosion of 5.9 t ha<sup>-1</sup> a<sup>-1</sup>), respectively. The black**  
 113 **rectangle in the catchment marks the section of the detailed maps in Fig. 7.**  
 114

115 *2.2. Model*

116 The erosion and MP transport is modelled based on a modified version of the spatially distributed  
 117 water and tillage erosion and carbon (C) turnover model SPEROS-C (Fiener et al., 2015; Van Oost et  
 118 al., 2005a). SPEROS-C was deliberately selected as (i) it allows the spatially explicit integration of yearly  
 119 MP inputs since 1950, (ii) it routes sediment and MP through the landscape while including deposition of

120 both, and (iii) it includes water and tillage erosion as well as a yearly soil profile update (10 layers of 10  
121 cm thickness) accounting for changes in MP allocation following erosion or deposition. Both, the  
122 modeled deposition and the MP soil profile update allow us to analyze potential MP landscape sinks  
123 either in space (e.g., in grassed areas) or in depths below the plough layer, where MP is not affected by  
124 water erosion anymore.

125 The model was originally developed to analyse the long-term effect of soil erosion on landscape-scale  
126 carbon balance (e.g. Nadeu et al., 2015), whereas the erosion components are based on the erosion and  
127 sediment transport model WaTEM/SEDEM, which was extensively tested and validated in different  
128 regions of the world (Krasa et al., 2005; Van Oost et al., 2000; Van Rompaey et al., 2001; Verstraeten  
129 and Prosser, 2008). The most important model components for this study are: (i) the water erosion and  
130 sediment transport component, (ii) the tillage erosion component, and (iii) the lateral redistribution and  
131 the vertical mixing of MP in the soil profile following erosion and deposition processes. The model  
132 component responsible for C turnover was not used and focuses exclusively on the erosion, transport,  
133 and deposition of C as MP, taking into account the spatially differently distributed MP inputs from  
134 different MP sources. As a result of these changes, the model is referred to as SPEROS-MP for the  
135 purposes of this study. Based on the model structure it cannot account for particle size-specific selective  
136 erosion, and hence, the model does not consider preferential erosion of plastic particles, depending on  
137 the size, shape, density, etc. of different polymers. However, the model can account for different transport  
138 pathways of different MP input sources e.g., routing tyre wear from fields along streets throughout to  
139 catchment to the stream network.

140 *Water erosion component:* The water erosion component of SPEROS-MP consists of two main parts.  
141 First, the erosion potential of each raster cell (5 m x 5 m) is estimated based on the German version of  
142 the Universal Soil Loss Equation ABAG (Schwertmann et al., 1987). The major advantage of this well-



143 tested approach is that the input data to calculate the different USLE (ABAG) factors are available from  
 144 the Bavarian State Office of Agriculture (Bayerische Landesanstalt für Landwirtschaft; LfL) and are  
 145 regularly updated by the State Office administration. Sediment transport per raster cell, and hence  
 146 deposition if transport capacity is smaller than sediment influx, is calculated using Eq. 1:

$$147 \quad T_c = k_{tc} \cdot R \cdot C \cdot K \cdot LS_{2D} \cdot P \quad (\text{Eq. 1})$$

148 Where  $T_c$  is the transport capacity ( $\text{kg m}^{-1} \text{a}^{-1}$ ),  $k_{tc}$  is the transport coefficient;  $R$  ( $\text{N h}^{-1} \text{a}^{-1}$ ),  $C$  (-),  $K$  ( $\text{kg}$   
 149  $\text{h m}^{-2} \text{N}^{-1}$ ) and  $P$  (-) are the rainfall erosivity, soil cover, soil erodibility, and management factors of the  
 150 USLE calculated for Bavaria following the approach of Fiener et al. (2020).  $LS_{2D}$  is a grid cell-specific  
 151 topographic combined slope gradient and lengths factor calculated following Desmet and Govers (1996,  
 152 using the digital elevation model (DEM) with a resolution of 5 m x 5 m.

153 *Tillage erosion component:* Tillage erosion is calculated based on a diffusion-type equation adopted  
 154 from Govers et al. (1994), which generally assumes that tillage erosion is proportional to slope gradient  
 155 (Van Oost et al., 2006):

$$156 \quad Q_{til} = -k_{til} \frac{\Delta h}{\Delta x} \quad (\text{Eq. 2})$$

157 where  $Q_{til}$  is the soil flux in  $\text{kg m}^{-2} \text{yr}^{-1}$ ,  $\Delta h$  is the elevation difference in metres,  $\Delta x$  is the horizontal  
 158 distance in meters, and  $k_{til}$  is the tillage transport coefficient in  $\text{kg m}^{-1} \text{yr}^{-1}$ :

$$159 \quad k_{til} = BD_i \cdot TD_i \cdot x_{til} \quad (\text{Eq. 3})$$

160 where  $x_{til}$  is the tillage translocation distance in meters,  $BD_i$  is the soil bulk density in  $\text{kg m}^{-3}$ ,  $TD_i$  is  
 161 the vertical depth of tillage depth (20 cm). It is important to note that tillage erosion has no direct effect  
 162 on sediment or MP delivery into the stream network, but over time it modifies the MP concentration in

163 the plough layer of different raster cells, leading to a decrease in MP delivery, because at erosional sites  
164 subsoil with little potential MP is mixed into the plough layer, while MP at depositional sites is buried  
165 below the plough layer.

166 *MP redistribution and vertical mixing:* It is generally assumed that MP is entering the soil via its  
167 surface and is immediately mixed into the plough layer (upper 0.2 m). The MP input to arable land is  
168 estimated at field level (see input estimate below). For MP erosion the concentration in the plough layer  
169 of each 5 m x 5 m raster cell was multiplied with the bulk soil erosion of this raster cell to calculate the  
170 MP outflux to neighbouring cells. The MP concentration of the transported sediment is analogously used  
171 to calculate potential MP deposition. After each year of modelling water and tillage erosion, the soil  
172 profile is updated assuming a tillage operation to a constant depth of 0.2 m. Consequently, MP-free  
173 subsoil is mixed into the plough layer at erosional sites, decreasing the topsoil MP concentration, while  
174 at depositional sites the deposited MP is mixed with the underlying old plough layer, creating a new  
175 topsoil MP concentration and some MP in the layer no longer reached by the plough. Over the years this  
176 creates a steadily increasing variability in MP concentration within fields and transports MP into soils of  
177 other land uses (e.g. grassland and forest sites) assumed not to get other MP inputs.

## 178 2.3. Data

### 179 2.3.1. Soil erosion model inputs and parameters

180 For the study area, the LfL provided a digital elevation model (DEM, raster 5 m x 5 m), land-use data  
181 (field based), and a soil map (1:25,000) as well as most USLE factors (Tab. 1). For the sake of simplicity  
182 and because long-term data on soil management was missing, only the rainfall erosivity (*R* factor of the  
183 USLE) was calculated yearly. Therefore, we followed the approach of Schwertmann et al. (1987) using  
184 a relation between annual rainfall erosivity and mean annual precipitation. Based on annual precipitation  
185 available in a 1 km x 1 km grid resolution from the German Weather Service (DWD, 2020), yearly *R*

186 factor maps were created as model input. It is therefore important to note that the variation in model  
187 sediment fluxes is solely a result of varying the annual rainfall erosivity, while changes in land  
188 management (affecting the  $C$  factor of the USLE) are not considered. However, the primary focus of the  
189 study was to showcase the potential magnitude and variation of MP delivery, also affected by varying  
190 MP input in space and time since 1950. We assumed a corn-grain crop rotation (with a mixture of small  
191 grain crops and a proportion of row crops of 25%) typically found in the region and used the USLE  
192 calculator developed by Brandhuber et al. (2018), resulting in a  $C$  factor of 0.15, which is constantly  
193 used for all arable land in the catchment (Tab. 1). Routing sediments from arable land to the stream  
194 network, requires a sediment transport through other land uses, like forest, grassland, or paved surfaces.  
195 Therefore, these land uses need to be part of the erosion modelling and hence also require a  $C$  factor. For  
196 forest and grassland, a low  $C$  factor of 0.004 and for paved surfaces a  $C$  factor of 0.001 was applied  
197 (Brandhuber et al., 2018). A  $K$  factor map was provided by the LfL (derived from the soil properties  
198 given by the soil overview map of Bavaria at a scale of 1:25,000) based on the calculation in  
199 Schwertmann et al. (1987). The  $LS_{2D}$  factor was derived from the 5 m x 5 m DEM, following the approach  
200 of Desmet and Govers (1996). Assuming some soil conservation methods to be in place, e.g. partial  
201 contour ploughing, the  $P$  factor was set to 0.85 (Fiener et al., 2020).

202 The values of the transport capacity coefficient  $k_{tc}$  for different land use types must be generally  
203 determined through calibration or taken from calibrated literature values (Dlugoß et al., 2012). Based on  
204 an extensive study of Van Oost et al. (2003), who tested the sensitivity of the transport capacity  
205 coefficient for different arable land and different raster resolutions, an optimum value in case of a 5 m x  
206 5 m grid resolution of  $k_{tc} = 150$  m was determined, which is used in this study. The author (Van Rompaey  
207 et al., 2001) identified favorable  $k_{tc}$  values ranging between 0 and 60 for non-erosive landscapes at a  
208 20x20 m grid, with an optimum at 42. Given my use of a finer 5x5 m grid resolution, scaled down by a  
209 factor of 4, a  $k_{tc}$  value of 10 was estimated for forest and grassland.

210 The tillage transport coefficient  $k_{til}$  depends on the tillage implement, tillage speed, tillage depths, bulk  
 211 density, texture and soil moisture at time of tillage (Van Oost et al., 2006). For the tillage erosion  
 212 modeled, a constant  $k_{til}$  value of  $350 \text{ kg m}^{-1} \text{ a}^{-1}$  for all fields was assumed (Tab. 1), which is a conservative  
 213 estimate of a mixture of mouldboard and chisel ploughing (Van Oost et al., 2006).

214 **Table 1: Model parameters used in SPEROS-MP.**

Parameters	Value	Unit	Comment	Reference
$R$	0.048- 0.089	$\text{N h}^{-1} \text{ a}^{-1}$	Varies annually, <b>controls the variability of the model</b>	<i>DWD (2020)</i>
<i>C</i>				
<i>Arable land</i>	0.15	-	Does not vary spatially within different land uses	<i>Brandhuber et al., 2018</i>
<i>Forest and grassland</i>	0.004	-		
<i>Urban area</i>	0.001	-		
$K$	5-55	$\text{kg h m}^{-2} \text{ N}^{-1}$	Varies spatially depending on soil texture	<i>Fiener et al., 2020</i>
$P$	0.85	-		<i>Fiener et al., 2020</i>
<i>ktc</i>				
<i>Arable land</i>	150	<i>m</i>	Does not vary spatially within different land uses	<i>Dlugoß et al., 2012</i>
<i>Forest and grassland</i>	10	<i>m</i>		<i>Van Rompaey et al., 2001</i>
<i>Urban area</i>	0	<i>m</i>		
$k_{til}$	350	$\text{kg m}^{-1} \text{ a}^{-1}$		<i>Van Oost et al. 2006</i>

215

### 216 2.3.2.MP contamination of soils

217 Because sampling and sample analysis would be extremely time consuming and costly, it is not  
 218 possible to determine the actual MP concentrations in a  $390 \text{ km}^2$  catchment where estimates from MP  
 219 inputs suggest large spatial heterogeneity. Hence, the potential soil-MP contamination needs to be  
 220 estimated from the potential MP input from different sources. As soil erosion is dominant on arable land,  
 221 an exclusive input estimate was performed for arable land. However, it is important to emphasize that,  
 222 except for tyre wear, estimates are based on regional means for the whole of Bavaria and that in general  
 223 estimates of the MP accumulated in the catchment soils since the 1950s needs a number of assumptions

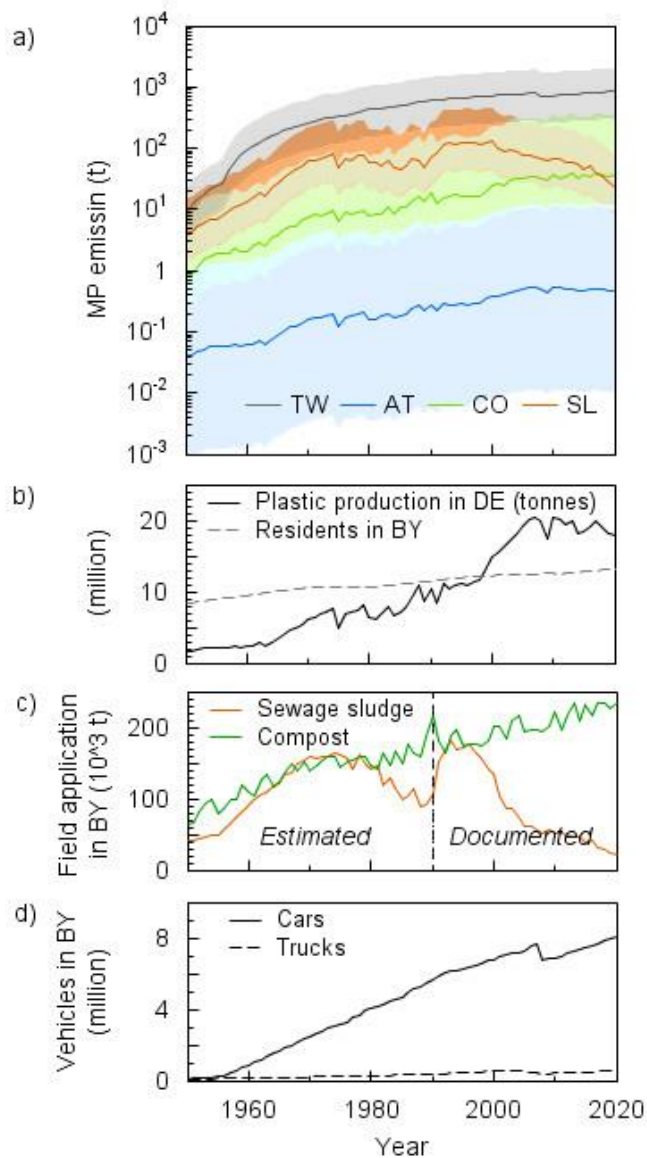
224 and simplifications, resulting in large uncertainties regarding the MP concentrations in soils. To account  
225 for these uncertainties in the model outputs and arrive at a robust indication of the potential contribution  
226 of soil erosion as a source of MP in the stream network, we estimated the potential yearly mean,  
227 minimum and maximum soil-MP input for each input pathway (see below) and did separate and  
228 combined modelling runs for the different contamination estimates. As mentioned earlier, mean MP  
229 inputs from sewage sludge, compost and atmospheric deposition were estimated from means for all  
230 arable land in Bavaria, while input of tyre wear was derived using catchment specific road data and road  
231 specific traffic data as far as possible. These represent the typical sources in the agricultural landscape  
232 of Southern Germany, along with MP, applicable for SPEROS-MP. Other potential MP input pathways,  
233 for instance from plastic used in agricultural management (e.g. mulch films) or from littering, were not  
234 considered for two main reasons. (i) In Bavaria mulch films are mostly associated with certain regions  
235 where specific crops or vegetables are grown, especially asparagus. For our test site this is not the case,  
236 and using the average area of mulch cover in Bavaria to estimate the potential mean input in the  
237 catchment would have resulted in very small input amounts, not comparable with other regions in the  
238 world, where mulch films can be a very important source of MP (Li et al., 2022; Liu et al., 2014). (ii)  
239 Larger macroplastic fragments from mulch films and littering should only be transported with severe rill  
240 and ephemeral gully erosion, which are not the dominant erosion processes in the region.

### 241 *2.3.3. Sewage sludge and compost*

242 Sewage sludge and compost as soil amendments (organic fertilizers) contain different quantities of  
243 microplastic and, in the case of compost, small macroplastic. The first step was to estimate the amount  
244 of sewage sludge and compost applied on Bavarian agricultural soils since 1950. Bavarian waste reports  
245 (LfU, 1990-2020) allowed us to determine the mean annual input on arable land for the time period  
246 1990–2020. Historical application rates of compost were determined based on a linear relationship

247 between application rates and population numbers between 1990 and 2020 (the variability was continued  
248 at random) (LfStaD, 2022) (Fig. 2b, c). In the case of sewage sludge, the number of residents connected  
249 to the sewage system was taken into account (Schleypen, 2017). The gaps between historical individual  
250 values were interpolated. The development of plant technology and the use of sewage sludge between  
251 1945 and 1990 were considered, as described by Schleypen (2017). While compost was constantly used  
252 as an organic fertilizer, the use of sewage sludge was quite variable over time (Fig. 2c). From 1970  
253 onwards new wastewater treatment plant (WWTP) technology meant that the sewage sludge was no  
254 longer allowed to accumulate dry, but rather as wet sludge (Schleypen, 2017). This led to a sharp drop  
255 in the use of sewage sludge as a fertilizer and it was not until the 1990s that it become popular again  
256 (Fig. 2c). Since 2017, the application of sewage sludge has been largely banned in Bavaria (Schleypen,  
257 2017).

258 The second step was to estimate the MP concentrations in sewage sludge and compost. To do this,  
259 current literature values were used to estimate the MP concentrations for 2020. A minimum, mean and  
260 maximum MP concentration was always considered, based on the range of values from literature. For  
261 sewage sludge, data from Edo et al. (2020) were used; this is, to our knowledge, one of the few studies  
262 providing a mass balance of MP for a WWTP by specifying the total wastewater volume and the total  
263 amount of sewage sludge per day. The sum of the MP particles filtered out (contained in sewage sludge)  
264 and the delivered MP from the WWTP effluent results in the number of MP detected in the WWTP input.  
265 Edo et al. (2020) consider size classes 25–104  $\mu\text{m}$ , 104–375  $\mu\text{m}$  and 375–5,000  $\mu\text{m}$  and their data show  
266 that 95% of the MP in the WWTP is retained in the sewage sludge, which is consistent with other  
267 publications giving ranges of 93–98% (Habib et al., 2020; Tang and Hadibarata, 2021; Unice et al.,  
268 2019). For compost, data from Braun et al. (2021) were used, which contain all essential data on MP in  
269 compost from Germany. They examined MP in the size ranges  $< 1,000 \mu\text{m}$ , 1,000–5,000  $\mu\text{m}$  and  $> 5,000$   
270  $\mu\text{m}$ . For the mass calculation of the MP in compost, macroplastics are also included.



271  
 272 **Figure 2: a) The MP emissions for arable land in Bavaria from the different sources, tyre wear**  
 273 **(TW), sewage sludge (SL), compost (CO) and atmospheric deposition (AT), from 1950 to 2020. b)**  
 274 **The development of plastics production in Germany and the population of Bavaria since 1950. c)**  
 275 **Amount of application of sewage sludge and compost as fertilizer on Bavarian arable land. d)**  
 276 **The number of registered cars and trucks in Bavaria since 1950.**

277

278 Both publications, Edo et al. (2020) and Braun et al. (2021), provide information on the size  
279 distribution of the detected MP particles. This enabled the most accurate conversion possible between  
280 mass and particle number. When converting, the particle size, size distribution and shape were taken into  
281 account. While a spherical shape was assumed for sewage sludge, for compost the most realistic possible  
282 volume for each detected particle was calculated (individual dimensions have been provided by the  
283 authors of Braun et al. (2021). Based on the type of plastic detected, an average density of 1 was assumed  
284 for all particles. An average MP load of 1.14 g MP kg<sup>-1</sup> dry matter of sewage sludge (min.: 0.42 g, max.:  
285 4.04 g) and 0.15 g MP kg<sup>-1</sup> dry matter of compost (min.: 0.05 g, max.: 1.36 g) was assumed.

286 Based on the known amounts of sewage sludge and compost applied, it was possible to calculate the  
287 corresponding amount of MP that ends up on Bavarian agricultural soils (kg m<sup>-2</sup>). When calculating the  
288 MP concentration back to 1950, the amount of plastic produced in Germany was considered for each  
289 year, as the MP concentration depends on the level of production (Fig. 2a, b). The annual amount of MP  
290 was then evenly distributed across all agricultural fields in Bavaria, since spatial allocation within the  
291 study area was not possible. Due to the lack of parcel-specific information before 2015 for sewage  
292 sludge, we estimated MP inputs using average values per field, similar to compost. However, primary  
293 aim in this modelling exercise wasn't to precisely replicate MP delivery in the Glonn catchment. Instead,  
294 to demonstrate the model's use in a system analysis, acknowledging limitations in historical data  
295 availability.

296 Between 1950 and 2020, a total of 7.26 million tonnes of sewage sludge and 11.7 million tonnes of  
297 compost were added as organic fertilizer on agricultural fields in Bavaria. Hence it can be estimated that  
298 4,090 t (min.: 1,510 t, max.: 14,500 t) and 1,110 t (min.: 358 t, max.: 10,100 t) of MP from sewage sludge  
299 and compost, respectively, was dumped on arable land in Bavaria. From that, an average input on the  
300 arable land in the Glonn River catchment of 42,100 kg MP from sewage sludge (min.: 15,500 kg, max.:



301 149,000 kg) and 11,500 kg MP from compost (min.: 3,660 kg, max.: 104,000 kg) was calculated. For  
302 the arable land in the Glonn River catchment, this means an average annual MP application of 240 kg  
303 MP from sewage sludge (min.: 90 kg, max.: 860 kg) and 370 kg from compost (min.: 120 kg, max.:  
304 3,390 kg) in 2020 (Tab. 2). This results in a current entry rate of 1.14 mg MP m<sup>-2</sup> a<sup>-1</sup> (min.: 0.42 mg, 4.04  
305 mg) from sewage sludge and 1.75 mg MP m<sup>-2</sup> a<sup>-1</sup> (min.: 0.56 mg, max.: 15.8 mg) from compost.

#### 306 *2.3.4. Atmospheric deposition*

307 For the atmospheric deposition of MP, the data from four bulk deposition measurements (precipitation  
308 and dust deposition) in Bavaria (Witzig et al., 2021) were combined with the development of plastics  
309 production in Germany since the 1950s. Historically, the calculation of MP load relied on the assumption  
310 that increased plastic production corresponds to higher emissions (Fig. 2a), although this approach is  
311 notably simplified. This results in a mean cumulative atmospheric MP input on arable land in Bavaria of  
312 18 tons of MP (min.: 0.41 t, max.: 407 t). Between 1950 and 2020, the arable land in the Glonn River  
313 catchment was loaded with a total of 186 kg of MP (min.: 4.20 kg, max.: 4,200 kg). For 2020 an average  
314 annual MP immission of 4.76 kg (min.: 0.11 kg, max.: 107 kg) or 0.02 mg MP m<sup>-2</sup> a<sup>-1</sup> (min.: 0.0005 mg,  
315 max.: 0.5 mg) via atmospheric deposition was calculated (Tab. 2).

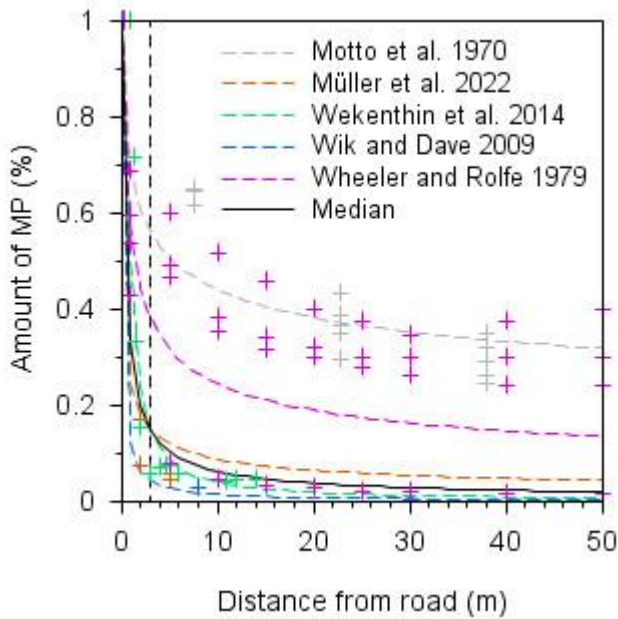
#### 316 *2.3.5. Tyre wear*

317 To determine the tyre wear particle input in the Glonn catchment we used existing traffic counting data  
318 from 2005, 2010 and 2015 for the main roads (motorways, federal roads, state roads and district roads)  
319 available from the Bavarian Road Information System (BAYSIS, 2015). Traffic volume for smaller roads  
320 (except farm roads) in rural areas were derived from a 1 km x 1 km population density grid following  
321 Gehrke et al. (2021). Based on these data the traffic volume (number of vehicles per km) for each paved  
322 road in the Glonn catchment could be estimated for the years 2005, 2010 and 2015. This was done

323 separately for passenger cars (cars), heavy-duty vehicles (trucks) and motorcycles. For all other years,  
324 the traffic volume (number of vehicles per km) per road was linearly extrapolated based on the traffic  
325 volume in and the number of registered cars and trucks in Bavaria (LfStaD, 2022) (Fig. 2d). No emissions  
326 from unpaved roads and agricultural machinery were considered.

327 A minimum, medium and maximum scenario was considered, based on the quantity of released tyre  
328 particles specified in the literature. A mean tyre wear emission factor of 90 mg TW km<sup>-1</sup> (min.: 53 mg,  
329 max.: 200 mg) was assumed for cars (a motorcycle represents half a car) and 700 mg TW km<sup>-1</sup> (min.:  
330 105 mg, max.: 1,7\*10<sup>3</sup> mg) for trucks, based on the reviews of Hillenbrand et al. (2005) and Wagner et  
331 al. (2018). Based on the length (km) and traffic volume (number of cars, motorbikes and trucks), the  
332 released TW was calculated for each section of road.

333 The transport of TW from roads into the surrounding soil systems was estimated based on literature  
334 information, assuming that the TW concentration exponentially declines with increasing distance from  
335 the road (Fig. 3). However, we could only identify one study (Müller et al., 2022) that directly measured  
336 TW contamination of soils with distance from the road, while most other studies (Motto et al., 1970;  
337 Werkenthin et al., 2014; Wheeler and Rolfe, 1979; Wik and Dave, 2009) used chemical markers and the  
338 distance from the road to estimate TW distribution. From all these different approaches we calculated a  
339 median behaviour (Fig. 3). As the modelling is performed in a 5 m x 5 m grid, the land-use map may not  
340 show all grass or vegetation strips often found along roads, which might lead to an overestimation of  
341 TW input to arable land. Hence, we decided to use a conservative estimate, assuming that at least a 3 m  
342 wide grass strip can be found on both sides of any road. Consequently about 85% of the TW produced  
343 on any road (Fig. 3) cannot reach arable fields. The remaining 15% of TW that could potentially reach  
344 arable land mostly settles within a 50 m distance from the road, whereas background MP concentrations  
345 are reached in about 130 m distance (Fig. 3).



346  
 347  
 348 **Figure 3: The distribution of tyre wear in the soil relative to the distance from the road. Literature**  
 349 **values are based on direct detection of tyre wear (Müller *et al.* 2022) or on the estimated**  
 350 **concentrations of tyre wear particles based on chemical markers (Motto *et al.* 1970, Wheeler and**  
 351 **Dave 2009; Wik and Dave 2009; Wekenthin *et al.* 2014). The markers show the individual values,**  
 352 **the dashed lines show the mean of the respective reference. The black line represents the median**  
 353 **of all literature values used for modelling in this study.**

354  
 355 In comparison to the other MP sources considered (sewage sludge, compost and atmospheric deposition),  
 356 the estimate for TW was calculated on a field-by-field basis. To identify all agricultural fields affected  
 357 by road-borne TW deposits within a distance of 130 m, a land-use map was overlaid on the road network.  
 358 For each field, the area share of the associated road section and the distance to the road were considered  
 359 when calculating the TW load. The only limitation is that on fields affected by TW, in the model the  
 360 amount of TW was then distributed evenly over the entire field and not just on the affected field section  
 361 near the road (within 130 m).

362 Between 1950 and 2020,  $120 \cdot 10^3$  kg tyre wear (min.:  $44 \cdot 10^3$  kg, max.:  $289 \cdot 10^3$  kg) ended up on  
 363 arable land in the Glonn catchment (Tab. 2). In 2020 the average annual MP application amounts to

364 3.1\*10<sup>3</sup> kg of tyre wear (min.: 1.1\*10<sup>3</sup> kg, max.: 7.5\*10<sup>3</sup> kg) (Tab. 2). The load from TW in 2020 can  
 365 reach maximum concentrations of 2.5\*10<sup>3</sup> mg TW m<sup>-2</sup> a<sup>-1</sup> on roads with heavy traffic use; the average  
 366 over all affected fields in the Glonn catchment area is 19.7 mg TW m<sup>-2</sup> a<sup>-1</sup> (Tab. 2).

367 **Table 2: MP inputs into arable soils within the test catchment, separated by different sources. All**  
 368 **values are listed for the modelled time span 1950–2020 and separately for the year 2020.**  
 369

	Tyre wear	Sewage sludge	Compost	Atmospheric deposition	Unit
<b>1950–2020</b>					
<b>MP application to arable land</b>	<b>120,256</b>	<b>42,100</b>	<b>11,500</b>	<b>186</b>	<b>kg</b>
min	43,969	15,500	3,660	4.30	
max	288,614	14,9000	104,000	4200	
<b>2020</b>					
<b>MP application to arable land</b>	<b>3,109</b>	<b>240</b>	<b>370</b>	<b>4.76</b>	<b>kg</b>
min	1,137	90	120	0.11	
max	7,462	860	3,390	107	
<b>MP application rate</b>	<b>19.67</b>	<b>1.14</b>	<b>1.75</b>	<b>0.02</b>	<b>mg MP m<sup>-2</sup> a<sup>-1</sup></b>
min	7.19	0.43	0.56	5*10 <sup>-4</sup>	
max	47.2	4.08	16.03	0.45	

370

#### 371 2.4. Model validation

372 It is obviously impossible to validate the modelled MP delivery to the stream network against measured  
 373 MP loads, as this would call for a continuous monitoring of MP delivery for several years at least.  
 374 However, the modelled sediment delivery can be validated against measured data from the Bavarian  
 375 State Office for Environment (Bayerisches Landesamt für Umwelt, LfU), which operated a discharge  
 376 and sediment monitoring gauge in Hohenkammer (Fig. 1) between 1968 and 2020. At this gauge with a  
 377 defined river cross-section, daily discharge was derived from continuous runoff depth measurements in  
 378 combination with a stage discharge rating curve, while the stationarity of this rating curve at the  
 379 measuring cross-section was randomly checked once or twice every year. At the gauging station a weekly

380 water sample was collected (1968–2020) and its sediment concentration was determined in the  
381 laboratory. From 2011 onwards a turbidity probe (Solitax ts-line; Hach Lange GmbH; Germany) was  
382 installed and regularly calibrated against the samples taken by hand. Based on the continuous discharge  
383 and the weekly to continuous sediment concentration measurements, the LfU provided daily sediment  
384 load data for the time span 1968 to 2020, which were aggregated to yearly values for this study.

## 385 2.5. Modelled scenarios

386 Apart from modelling and analysing the MP delivery to the stream network via the erosion pathway  
387 for the period from 1950 to 2020, we also modelled three scenarios (S1 to S3) to discuss potential future  
388 pathways up to 2100.

389 *Scenario S1 – business-as-usual scenario:* In this scenario it is assumed that the MP input to arable  
390 land continues until 2100 with the same input rates estimated for 2020. Given the ongoing increase in  
391 plastics production (Chia et al., 2021; Lwanga et al., 2022) and rising traffic numbers (StMB, 2023), this  
392 may even be a conservative estimate of a business-as-usual scenario pathway.

393 *Scenario S2 – spatially targeted application of soil amendments:* This scenario addresses two aspects.  
394 (i) A potential reduction of MP delivery to the stream network due to a targeted application of soil  
395 amendments, keeping a distance of at least 100 m from the stream network in the case of compost and  
396 sewage sludge application. (ii) More generally illustrating the sensitivity of MP delivery to the stream  
397 network in the case of non-homogenous MP inputs in the catchment. For the latter, soil amendments  
398 were solely applied in the vicinity of the stream network (max distance 100 m).

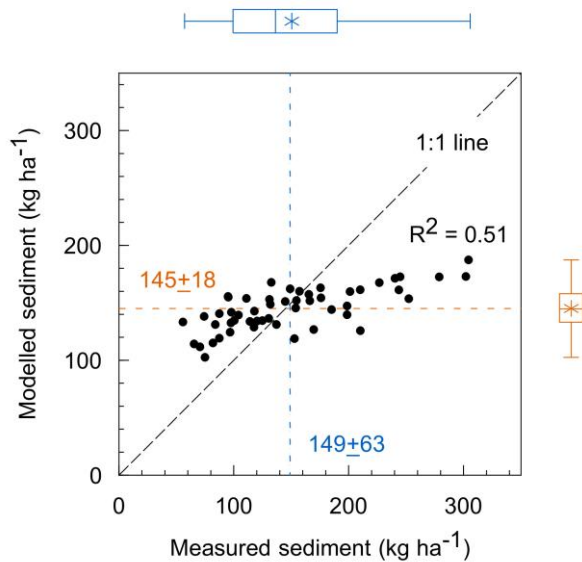
399 *Scenario S3 – stop MP input:* This scenario is set up to determine the extent to which soils function  
400 as a long-term source for MP with regard to soil erosion, assuming the MP applied before 2020 remains  
401 stable in the soil until 2100. Therefore, a potential decline in MP concentration in the plough layer either

402 results from a lateral loss to neighbouring land uses (grassland or forest) or the stream network, or is  
403 buried below the plough layer due to deposition processes (here deposition due to water and tillage  
404 erosion).

### 405 **3. Results**

#### 406 *3.1. Sediment delivery*

407 Without any calibration, the model satisfactorily reproduced the measured long-term mean sediment  
408 delivery of the Glonn outlet (Fig. 4). The modelled sediment deliveries resulted in a mean of  $145 \pm 18$  kg  
409  $\text{ha}^{-1}$ , the measured mean contained  $149 \pm 63$  kg  $\text{ha}^{-1}$  kg  $\text{ha}^{-1}$  (Fig. 4). The model was obviously not able to  
410 capture the full variability in the measured yearly sediment delivery ( $R^2 = 0.51$ ; Fig. 4). It underestimates  
411 years with high erosion rates, while it overestimates years with low erosion rates. However, we conclude  
412 that the model performance (especially in reproducing the long-term mean) gives a solid basis for  
413 modelling lateral MP fluxes due to erosion processes. Here it is important to note that our modelling  
414 approach aims to estimate the magnitude of the MP erosion transport pathway, which was not analysed  
415 in earlier studies, and that the estimated MP inputs contribute significantly to model uncertainty.



416  
 417 **Figure 4: Measured and modelled sediment delivery (1968 to 2020) at the outlet of the Glonn**  
 418 **catchment. The blue and orange lines represent the measured and modelled means, respectively.**  
 419 **The boxplots show the variability of the data. They show the median (line) and mean (star) and**  
 420 **the 1st and 3rd quartile, whiskers give the minimum and maximum.**

421  
 422 *3.2. MP erosion and delivery to stream network*

423 The constantly rising MP input to arable soils from different sources (Fig. 2) since 1950 is reflected  
 424 in the steadily increasing, erosion-induced MP delivery into the stream network (Fig. 5a). Due to the  
 425 long-term fertilization of arable land with sewage sludge, on average 0.51 kg of MP a<sup>-1</sup> entered the Glonn  
 426 stream network in 2020 (Tab. 3). For compost it is 0.77 kg of MP a<sup>-1</sup>, with 0.01 kg of MP a<sup>-1</sup> from  
 427 atmospheric deposition (Tab. 3, Fig. 5a). With compost, sewage sludge and atmospheric deposition as  
 428 potential MP inputs to arable land, SPEROS-MP generated a total MP input into the stream network of  
 429 1.29 kg MP via the soil erosion pathway in 2020. Deliveries to the stream network have also steadily  
 430 increased in terms of TW (Fig. 5a), with an average 5.04 kg of MP a<sup>-1</sup> delivered to the stream network  
 431 in 2020 (Tab. 3).

432

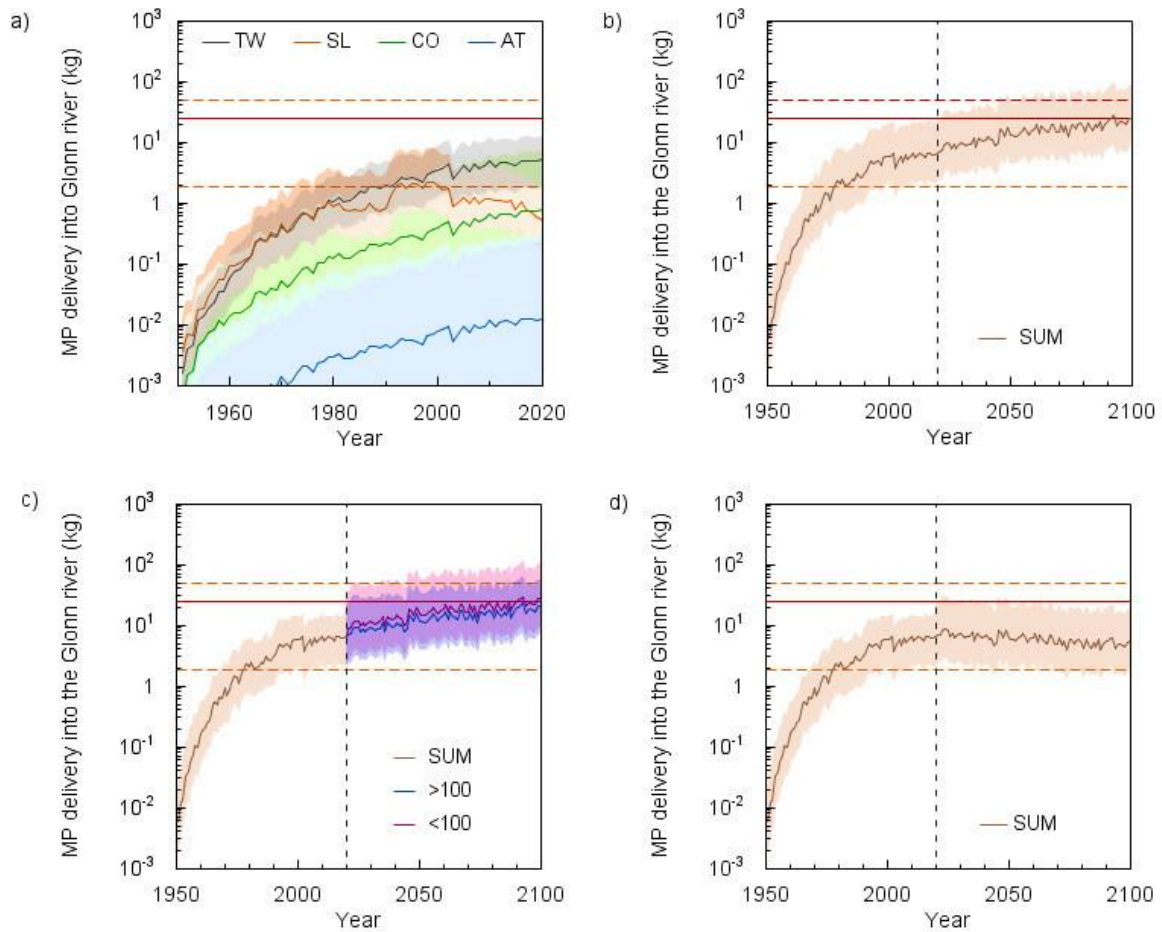
433 **Table 3: Soil erosion-induced MP delivery to the Glonn stream network, as well as redistribution**  
 434 **to grassland and forest. The MP vertical loss below the plough layer is also given. All values are**  
 435 **listed for the modelled time span 1950–2020 and separately for the year 2020.**  
 436

	Tyre wear	Sewage sludge	Compost	Atmospheric deposition	Unit
<b>1950–2020</b>					
<b>MP delivery into stream network</b>	<b>134</b>	<b>57</b>	<b>17</b>	<b>0.32</b>	<b>kg</b>
min	49.0	21	5	0.01	
max	322	200	155	9	
<i>Percentage of MP application</i>	<i>0.11</i>	<i>0.14</i>	<i>0.15</i>	<i>0.17</i>	<i>%</i>
<b>MP delivery into grassland</b>	<b>604</b>	<b>442</b>	<b>82</b>	<b>1.5</b>	<b>kg</b>
min	221	163	24	0	
max	1,450	1,551	748	42	
<i>Percentage of MP application</i>	<i>0.50</i>	<i>1.05</i>	<i>0.71</i>	<i>0.81</i>	<i>%</i>
<b>MP delivery into forest</b>	<b>108</b>	<b>97</b>	<b>18</b>	<b>0.34</b>	<b>kg</b>
min	39.5	36	5	0	
max	259	340	164	10	
<i>Percentage of MP application</i>	<i>0.09</i>	<i>0.23</i>	<i>0.16</i>	<i>0.18</i>	<i>%</i>
<b>MP loss below plough layer</b>	<b>4,703</b>	<b>2605</b>	<b>489</b>	<b>14.8</b>	<b>kg</b>
min	1,720	961	144	6	
max	11,287	9,414	4,458	386	
<i>Percentage of MP application</i>	<i>3.91</i>	<i>6.19</i>	<i>4.25</i>	<i>8</i>	<i>%</i>
<b>2020</b>					
<b>MP delivery into stream network</b>	<b>5.04</b>	<b>0.51</b>	<b>0.77</b>	<b>0.01</b>	<b>kg MP a<sup>-1</sup></b>
min	1.84	0.2	0.2	0.0003	
max	12.1	1.8	7	0.3	

437

438





439

440 **Figure 5: MP delivery into the Glonn shown individually for tyre wear (TW), sewage sludge (SL),**  
 441 **compost (CO) and atmospheric deposition (AT) or the sum of TW, SL, CO and AT (SUM). The**  
 442 **dashed line gives the year 2020 as the starting point for different scenarios. For comparison, the**  
 443 **amount of MP delivery through wastewater treatment plants (WWTP) in 2020 is shown as a red**  
 444 **line (min. and max. as dotted lines). a) MP delivery into the Glonn river between 1950 and 2020.**  
 445 **b) Result of scenario S1 with the assumption that the MP input will continue as in 2020. For**  
 446 **comparison, the amount of MP delivery through wastewater treatment plants (WWTP) in 2020.**  
 447 **c) Result of scenario S2. Compost and sewage sludge are applied to arable land at a distance of >**  
 448 **100 m and < 100 m from water streams. d) Result of scenario S3 with no MP input at all from 2020**  
 449 **onwards.**  
 450

451 Between 1950 and 2020, 208.3 kg of MP (134 kg TW, 57 kg sewage sludge, 17 kg compost and 0.32  
452 kg atmospheric deposition) entered the Glonn stream network (Tab. 3), while overall a sediment load of  
453  $3.0 \cdot 10^8$  kg was delivered to the catchment outlet. TW was the main MP source, accounting for 64.3%,  
454 followed by sewage sludge with 27.4%, compost with 8.2% and atmospheric deposition with 0.1%.  
455 Taking into account the MP delivery relative to the MP input (i.e. total amount of MP input into soil in  
456 1950–2020 vs. total MP delivery into the stream network from 1950–2020), only 0.14% of the MP  
457 released to arable land was transported into the Glonn stream network. This differs slightly for the  
458 different MP sources, ranging from 0.17% for atmospheric deposition to 0.11% for tyre wear (Tab. 3).

459 The spatially distributed model also allowed us to quantify the relocation of MP between different  
460 land uses (an example is shown in Fig. 6f). The amount of MP delivered between 1950 and 2020 from  
461 arable land to grassland and forest is  $1.1 \cdot 10^3$  and  $0.2 \cdot 10^3$  kg, respectively (Table 3). The larger delivery  
462 to grasslands is particularly interesting, as these are mostly located along the stream network (see  
463 discussion).

464 SPEROS-MP not only gives information about the MP relocation between arable land and other land  
465 uses. The model also determines the amount of MP allocated below the plough layer (and thus out of  
466 reach of water erosion) at depositional sites (an example is shown in Fig. 6e). Between 1950 and 2020,  
467 3.9% of the TW supplied to arable land was moved below the plough layer (Tab. 3). This corresponds  
468 to  $4.7 \cdot 10^3$  kg MP or 35 times the amount reaching the stream network via water erosion. For sewage  
469 sludge it is 6.19% ( $2.6 \cdot 10^3$  kg), for compost 4.25% (489 kg) and for atmospheric deposition 8% (14.8  
470 kg). Consequently, much more MP was translocated into the subsoil than was transported into the Glonn.  
471 This transport into the subsoil was caused by water erosion (48.5%) and tillage erosion (51.5%).  
472 Conversely, up to 95% of the MP applied to arable soil over the past 70 years remains in the plough layer  
473 (infiltration and bioturbation excluded).



474

475 **Figure 6: Example of catchment segment (for location see Figure 1) illustrating microplastic (MP)**  
 476 **input on arable land and results of erosion modelling between 1950 and 2020. The maps show the**  
 477 **situation in 2020. a) Field-based land use. b) Total MP input from sewage sludge, compost and**  
 478 **atmospheric input (without TW) as mean value over all arable land. c) MP input from TW,**  
 479 **spatially distributed to individual arable fields. d) MP concentration below plough layer. e) MP**  
 480 **transported to other land uses via soil erosion. f) MP distribution after water and tillage erosion**  
 481 **on arable land. (DEM © Bayerische Vermessungsverwaltung)**  
 482

483        *3.3. Scenario S1 – business-as-usual*

484        If arable soils continue to be loaded with MP the same as in 2020, the annual MP delivery rate into the  
485        Glonn stream network will increase by a factor of 4 by 2100. In 2100, 25.2 kg MP a<sup>-1</sup> (min.: 9.03 kg;  
486        max.: 84.1 kg) through TW, compost, sewage sludge and atmospheric deposition would end up in the  
487        stream network (Fig. 5b). Between 1950 and 2100, this would make a total MP input of 1.32 \*10<sup>3</sup> kg MP  
488        (min.: 511 kg; max.: 4.7 \*10<sup>3</sup> kg) into the stream network.

489        *3.4. Scenario S2 – spatially targeted application of soil amendments*

490        In S2 MP inputs from atmospheric deposition and TW accumulation continued like in S1. However, the  
491        location where the organic fertilizer (sewage sludge and compost) was applied in the catchment was  
492        changed. All organic fertilizers were either applied at a distance of at least 100 m from the stream network  
493        or within a distance smaller than 100 m along the stream network.

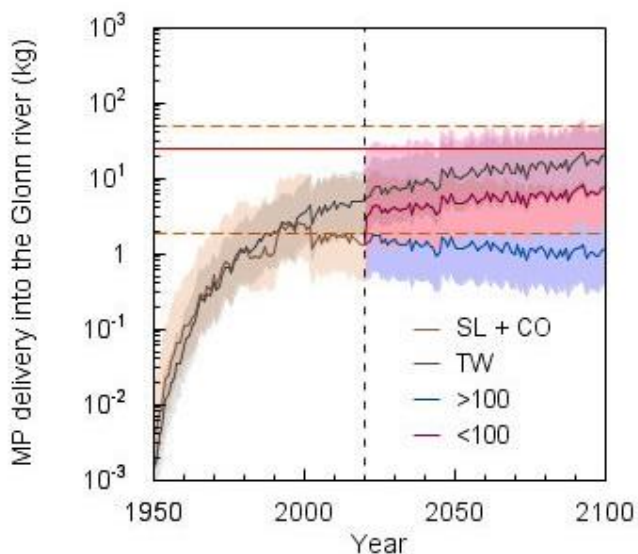
494        With an application at a distance of > 100 m, the MP delivery in the stream network would be reduced  
495        to a total of 21.2 kg (min.: 7.72 kg; max.: 55.9 kg) in 2100 (Fig. 5c). That would correspond to a reduction  
496        of 16% compared to S1. In the case of application at a distance of < 100 m, on the other hand, it would  
497        be 27.9 kg (min.: 10 kg; max.: 102 kg) in 2100 and thus an increase of 10.7% compared to S1 (Fig. 5c).

498        The result becomes clearer if we consider TW and the organic fertilizers separately. If the distance is >  
499        100 m, the annual MP delivery rate from organic fertilizer (sewage sludge and compost) without TW is  
500        1.1 kg MP a<sup>-1</sup> (min.: 0.4 kg, max.: 7.8 kg) in 2100 (Fig. 7). For 2100, this would result in a 78% reduction  
501        of the annual MP delivery rate from organic fertilizer into water bodies compared to S1. In total from

502 1950 to 2100, 173 kg MP (min.: 60 kg; max.:  $1.0 \cdot 10^3$  kg), or 46% less MP, from organic fertilizer would  
503 end up in the stream network until 2100 (the effect of atmospheric input is negligible).

504 If organic fertilizer is applied along the stream network (max. distance < 100 m), a MP delivery of 7.8  
505  $\text{kg a}^{-1}$  (min.: 2.6 kg, max.: 54 kg) is modelled in 2100 (Fig. 7). Between 1950 and 2100 a total of 493 kg  
506 MP (min.: 168 kg; max.:  $3.25 \cdot 10^3$  kg) would be delivered to the river system by organic fertilizer  
507 (without TW).

508



509 **Figure 7: Result of scenario S2 individually shown for tyre wear (TW) and for sewage sludge**  
510 **(SL) plus compost (CO) together as organic fertilizer applied to arable land at a distance of > 100**  
511 **m and < 100 m from water streams. For comparison, the amount of MP delivery through**  
512 **wastewater treatment plants (WWTP) in 2020 as red lines (min and max as dotted lines).**  
513  
514

### 515 3.5. Scenario S3 – stop MP input:

516 In scenario S3 MP input stops from 2020 onwards. This abrupt stop in plastic immission is not reflected  
517 in the MP delivery rates after 2020 (Fig. 5d). However, in the year 2100, 5.43 kg of MP  $\text{a}^{-1}$  (min.: 1.98  
518 kg, max.: 18.2 kg) would still end up in the stream network from arable land due to soil erosion (Fig.

519 5d). This corresponds to a decrease in the annual MP delivery rate of 14% between 2020 and 2100, with  
520 80 MP-free years (since 2020). Since 1950, a total of 684 kg MP (min.: 246 kg; max.:  $2 \cdot 10^3$  kg) would  
521 have ended up in the Glonn stream network.

522

## 523 **4. Discussion**

### 524 *4.1. Modelled erosion rates (sediment delivery)*

525 The modelling approach used, with a yearly time step and the missing temporal and spatial variability  
526 of most model input data (especially the constant crop cover factor), while only varying yearly rainfall  
527 erosivity, leads to model outputs that do not capture the full temporal dynamics of the measured yearly  
528 sediment delivery (Fig. 4). It is well documented that averaging model input variables over space and  
529 time generally leads to the overestimation of years with low sediment delivery and underestimation of  
530 years with high sediment delivery (Keller et al., 2021; Meinen and Robinson, 2021). The reduced  
531 temporal variability in modelled sediment delivery is expected for two main reasons: (1) the annual  
532 model time step averages out years where individual extreme events dominate the yearly sediment  
533 delivery, and (2) varying only the annual rainfall erosivity, while all other input parameters (especially  
534 cropping dynamics) are kept constant, cannot capture the temporal dynamics. However, without any  
535 model calibration the model is able to reflect the long-term mean sediment delivery between 1968 and  
536 2020 (Fig. 4), explaining 51% of the variability in the measured data. Hence, we conclude that SPEROS-  
537 MP is robust enough for this modelling study which focusses on MP delivery to the stream network in  
538 the Glonn catchment, especially as uncertainties associated with the erosion modelling are in any case  
539 smaller than the uncertainties associated with estimates of MP immissions to the arable soils in the  
540 catchment.

541 *4.2. Plausibility of MP soil input estimates*

542 Estimating the cumulative MP-soil immissions from different sources for a period starting from 1950  
543 is of course associated with large uncertainties. To account for these uncertainties, we deliberately used  
544 large ranges of possible inputs in our semi-virtual catchment approach which in the following discussion  
545 are compared with literature values for Germany or Bavaria as a whole.

546 *4.2.1. MP from sewage sludge, compost and atmospheric deposition*

547 Brandes et al. (2021) calculated mean MP inputs into agricultural soils in Germany for compost  
548 (1990–2016) and for sewage sludge (1983–2016). For Bavaria, their calculation results in compost-MP  
549 input rates of between 15 and 80 mg MP m<sup>-2</sup> a<sup>-1</sup> and sewage sludge-MP input rates between 0 and 190  
550 mg MP m<sup>-2</sup> a<sup>-1</sup>. Bertling et al. (2021) also determined MP immissions (TW excluded) to agricultural soils  
551 in Germany, resulting in much higher input rates for 2021 for compost and sewage sludge, with up to  
552 702 mg MP m<sup>-2</sup> a<sup>-1</sup> and 2.1\*10<sup>3</sup> mg MP m<sup>-2</sup> a<sup>-1</sup>, respectively. In contrast to the first authors, Braun et al.  
553 (2021) calculate the possible MP load for the legally permissible amount of compost applied to fields in  
554 Germany. This maximum permissible amount of compost application results in maximum possible entry  
555 rates ranging from 34 to 4.7\*10<sup>3</sup> mg MP m<sup>-2</sup> a<sup>-1</sup> into agricultural soils via compost.

556 For this study, an MP emission to arable soils of between 0.42 and 4 mg MP m<sup>-2</sup> a<sup>-1</sup> for sewage sludge  
557 and between 0.56 and 15.8 mg MP m<sup>-2</sup> a<sup>-1</sup> for compost were calculated for Bavaria. Our values are not  
558 based on the maximum possible limits, but on the most realistic estimates possible. Therefore, our MP  
559 loads remain well below the literature values. Nevertheless, the MP input from compost is likely to be  
560 underestimated, based on optical detection of MP > 1 mm (Bläsing and Amelung, 2018; Braun et al.,  
561 2021; Weithmann et al., 2018). Currently, much more compost (21\*10<sup>7</sup> t in 2020) is spread on fields in  
562 Bavaria than sewage sludge (24\*10<sup>4</sup> t in 2020), causing higher MP emissions from compost (Fig. 2a).

563 This results from the reduction in sewage sludge application, which has been largely banned in Bavaria  
564 since 2017 (Schleypen, 2017) (Fig. 2c). However, regional policy strategies regarding the use of sewage  
565 sludge differ substantially within Germany, making comparisons within the country somewhat difficult  
566 (Brandes et al., 2021).

567 For atmospheric deposition, an average of 771 and 395 MP particles  $\text{m}^{-2} \text{d}^{-1}$  were measured at rural  
568 locations in London and Hamburg (Klein and Fischer, 2019; Wright et al., 2019). Brahney et al. (2020)  
569 show that airborne microplastic particles accumulate at minimum concentrations of  $48 \pm 7$  MP particles  
570  $\text{m}^{-2} \text{d}^{-1}$  even in the most isolated areas of the United States (national parks and national wilderness areas).  
571 Even in Antarctic snow up to 29 MP particles per melted litre were found (Aves et al., 2022). In this  
572 study, the values of Witzig et al. (2021) were used to estimate the MP contribution via atmospheric  
573 deposition. They made MP measurements at different locations in Bavaria, ranging from  $74 \pm 19$  to  
574  $109 \pm 16$  MP particles  $\text{m}^{-2} \text{d}^{-1}$ . Even if the transfer of such particle numbers to mass inputs is associated  
575 with additional uncertainties, these amounts are orders of magnitude smaller than the inputs from sewage  
576 sludge and compost. In general, taking the considerable uncertainty in the data on MP inputs via the  
577 atmosphere into account, the results show that this magnitude is negligible compared to other sources  
578 investigated. This finding is important in a scientific context as it provides a better understanding of the  
579 magnitude of these inputs. The modelling analysis clearly shows that in comparison to other MP sources  
580 the atmospheric inputs are of minimal importance.

#### 581 *4.2.2. Tyre wear*

582 The large MP mass resulting from tyre wear is noticeable in both the TW input data and the TW  
583 delivery rates into the stream network. With modelled mean TW delivery of  $5 \text{ kg MP a}^{-1}$  in 2020 into the  
584 river system, the equivalent of half a car tyre ends up as MP in the Glonn (flow length of 50 km) each  
585 year. However, the calculated mean TW input to the Glonn catchment of  $200 \text{ mg MP m}^{-2}$  in 2020 is in



586 same the range as the estimates in other studies. For example, annual values of between 180 and 370 mg  
587 TW m<sup>-2</sup> were reported for Germany (Baensch-Baltruschat et al., 2020; Kocher et al., 2010; Wagner et  
588 al., 2018). The modelled MP input (see Fig. 3) to arable land in the Glonn catchment was substantially  
589 smaller, with a mean of 19.7 mg TW m<sup>-2</sup>.

590 Most of the TW remains on the roads or in the immediate vicinity. Some of the TW is expected to be  
591 transported directly into surface waters via runoff from the road. Baensch-Baltruschat et al. (2020)  
592 estimated that 12–20% of the tyre wear released on German roads ends up in surface water via road  
593 runoff. The hydrological model estimates of Unice et al. (2019) indicated that 18% of released tyre wear  
594 was transported to freshwater in the Seine River catchment. In comparison, focusing on erosion of MP  
595 which was mixed into the plough layer, only 0.11% of the applied TW to arable soils from 1950 to 2020  
596 reached the river system. Although TW is the largest source of entry in our study, the MP flow to the  
597 stream network is overall a conservative estimate. This mostly results from our assumption that all roads  
598 are surrounded by a 3 m grass buffer strip (even if this was not shown in the 5 m x 5 m land-use raster  
599 map used), always trapping at least 85% of the TW emissions (Fig. 3). Yet even this conservative  
600 assumption is associated with high uncertainties. The width of the grass strip between the road and the  
601 field has an enormous impact on the MP emission. A 2 m wide buffer strip would still retain  
602 approximately 80% and a 1 m wide buffer strip approximately 65% of the TW emission (Fig. 3). Without  
603 any assumed grass buffer strips, the MP emission from TW would be 8 times higher. Ultimately, the  
604 spatially distributed tyre wear is still associated with uncertainties. The level of TW emissions into the  
605 environment (not just arable land) makes other MP sources almost negligible, especially in terms of MP  
606 saving strategies.

607 Overall, it can be concluded that our estimates of MP input to the Glonn catchment are in the same  
608 order of magnitude, or somewhat smaller, compared to most other studies, and hence should be more or

609 less reasonable, even if any estimates are associated with large uncertainties (e.g. extrapolating back to  
610 1950; the small number of studies available for estimating MP concentrations in sewage sludge and  
611 compost; errors when transferring particle numbers in particle mass etc.). However, an error in modelling  
612 the MP delivery into the stream network of the test catchment most likely results from the fact that mean  
613 application rates (sewage sludge, compost) for the whole of Bavaria were used (Fig. 6b), while only TW  
614 input was calculated on a catchment-specific basis (Fig. 6c). Again, it is important to note that the Glonn  
615 catchment was used as an example to address and discuss the potential magnitude of the MP/soil erosion  
616 pathway in such mesoscale catchments determined by arable land use.

617 It should be noted that TW as not-agriculture MP-source is of paramount importance compared to  
618 other MP sources, especially with respect to MP reduction measures. Not only for soil, but also for water  
619 bodies and probably all other environmental compartments. Measures to prevent MP in soil will have  
620 little noticeable effect if TW remains unchanged. This problem should be given more consideration in  
621 future studies and interpretation of results (Knight et al., 2020a; Knight et al., 2020b; Mennekes and  
622 Nowack, 2022).

#### 623 *4.3. The modelled fate of MP*

624 As a mass-balanced model, SPEROS-MP calculates the MP input in mass ( $\text{kg m}^2$ ) and not in particle  
625 numbers. Hence, the model does not consider the type, shape, density, size or chemical properties of the  
626 MP particles from different MP sources. It thus treats the erodibility of MP from all input pathways  
627 equally. However, it can be assumed that particle properties play a decisive role for the erosion-induced  
628 lateral transport, as well as for the potential vertical transport. Small MP particles should be translocated  
629 faster below the plough layer due to bioturbation and maybe infiltration (Li et al., 2021; Rehm et al.,  
630 2021; Waldschläger and Schüttrumpf, 2020). A subsequent reduction in MP concentration in the plough

631 layer will also reduce MP erosion. On the other hand, smaller MP particles might more strongly interact  
632 with soil organic or mineral particles, or might even be included in soil aggregates, hence are more likely  
633 transported as bulk soil. For example, Rehm et al. (2021) were able to demonstrate in a long-term plot  
634 experiment that smaller PE particles (53–100  $\mu\text{m}$ ) are less strongly enriched in delivered sediments  
635 compared to larger PE particles (250–300  $\mu\text{m}$ ). Such behaviour might change again with increasing  
636 particle size, because if particles transported with sheet flow are larger than the flow depths (mostly < 1  
637 mm), transport in suspension is no longer possible.

638 In general, the potential decrease in topsoil MP concentration due to infiltration and bioturbation is  
639 not accounted for in SPEROS-MP. Vertical MP transport via infiltration and bioturbation has been  
640 widely discussed and partially observed in earlier studies, e.g. (Rillig et al., 2017), while earthworms  
641 play an especially important role in directly transporting MP via digestion and excretion (Huerta Lwanga  
642 et al., 2017) or in preparing preferential flow pathways for MP leaching (Yu *et al.*, 2019). Ignoring these  
643 processes of vertical movement below the plough layer will potentially lead to a slight overestimation of  
644 the topsoil MP concentration in the modelling approach presented here.

645 SPEROS-MP not only delivers MP into the stream network, but also redistributes MP within the  
646 catchment and within the soil profile. As arable land in the catchment is mostly found on the upper  
647 slopes, and grassland in the flood plains, large amounts of MP are transported from arable land to  
648 grassland (Tab. 3). No tillage takes place in grassland, leading to high MP concentration in the topsoil.  
649 Along the main river in particular, grassland contaminated with MP (example shown in Fig. 6f) offers a  
650 high potential for MP loss during flood events. In the flood plains, the groundwater level is regularly  
651 close to the surface, hence the chance of MP leaching to the groundwater increases (Chia et al., 2021;  
652 Singh and Bhagwat, 2022; Viaroli et al., 2022).

653 This analysis not only sheds light on the model's impact on MP distribution in varied landscape  
654 contexts but also underscores the potential environmental repercussions. The study significantly  
655 advances scientific understanding and practical relevance by emphasizing long-term field experiments  
656 and meso-scale model analyses. Nevertheless, gaps persist in MP research, particularly concerning  
657 standardized detection methods and quantification of terrestrial MP pollution. Addressing these gaps  
658 requires extensive additional research to comprehensively grasp the scope of MP pollution across diverse  
659 environmental media and the entirety of the MP cycle. Substantial measurements and fundamental  
660 research in this domain are imperative to enhance process comprehension and refine model applications.

#### 661 *4.4. Soil erosion as a potential MP source for inland waters*

662 Comparing the annual MP input to arable land and the annual MP loss through soil erosion indicates  
663 that only a very small proportion ( $\leq 0.17\%$  since 1950) is delivered to the stream network. The loss rate  
664 of TW (0.11%) was the smallest compared to sewage sludge, compost and atmospheric deposition (Tab.  
665 3). This is because the TW was not applied to all fields, but only to the fields next to a road. The low  
666 percentage of input lost to the streams should not lead to the fallacy that MP transport via soil erosion is  
667 negligibly small (Schell et al., 2022; Weber et al., 2022). This becomes clearer when comparing the MP  
668 input from soil erosion with the MP input from wastewater treatment plants (WWTP) in the study area  
669 (Fig. 5). Based on the known number and size of the WWTPs in the study area and MP loads in German  
670 WWTPs from literature (Mintenig et al., 2014), the MP delivery into the Glonn through WWTP outlets  
671 can be estimated at an average of 25 kg MP a<sup>-1</sup> (min.: 1.9 kg, max.: 49 kg) in 2020 (Fig. 5). These values  
672 represent a maximum scenario since the calculations were based on the possible full capacities of the  
673 WWTPs. Within the test catchment, the MP delivery into the stream network was 6.3 kg MP a<sup>-1</sup> (min.:  
674 2.2 kg, max.: 21 kg) in 2020, but (S1, Fig. 5b) could reach 25.2 kg MP a<sup>-1</sup> (min.: 9 kg, max.: 84.3 kg) by  
675 the end of the century (Fig. 5b).

676 Rehm et al. (2021) have shown that due to its low density, MP is preferentially eroded and is enriched  
677 by up to a factor of four in delivered sediments. These potential enrichment effects were not included in  
678 SPEROS-MP. In addition, other MP input sources such as plastic used in agriculture (e.g. mulch films)  
679 and littering were not considered in this study. In this respect, the modelled MP delivery is therefore a  
680 conservative estimate. Overall, our results are in line with other, larger-scale model estimates for the  
681 Bavarian section of the Danube catchment, showing that the MP input via soil erosion into water bodies  
682 in rural areas outweighs the MP input of WWTP outlets (Witzig et al., 2021). It should therefore not be  
683 claimed that soil erosion for MP transport is negligible (Schell et al., 2022) while wastewater treatment  
684 plants are treated as a major MP source for inland waters (Cai et al., 2022; Eibes and Gabel, 2022;  
685 Murphy et al., 2016).

#### 686 *4.5. The MP sink function of soil results in a long-term MP source*

687 Today's MP pollution of arable land represents a long-term MP source for inland waters. With the  
688 model scenarios S1 and S3, this study was able to show that the MP discharge from arable soils into  
689 inland waters via soil erosion will still affect many generations to come, even if MP entry into the  
690 terrestrial environment could be avoided. Because of low MP loss rates ( $\leq 0.17\%$ ) via soil erosion and  
691 the stability of conventional plastic materials over centuries (Ng et al., 2018), the MP particles  
692 accumulate in the soil over the years. As most of the MP stays in the plough layer (Tab. 3), it is made  
693 available to surface runoff and erosion processes on a regular basis. After 80 years without MP input in  
694 S3, MP delivery from the soil decreased only by 14%. The MP concentration in the topsoil of arable land  
695 decreases over time due to lateral MP loss into the stream network or into neighbouring grassland and  
696 forest areas (example shown in Fig. 6f). The MP concentration in the topsoil also decreases since erosion  
697 incorporates MP-free subsoil and, on the other hand, MP gets below the plough layer at depositional sites

698 (outside the range of water erosion). It is important to note that tillage erosion plays an important role,  
699 as it supports the burial of MP below the plough layer (example shown in Fig. 6e).

700 S3 is reminiscent of other well-known environmental problems of long-term diffuse pollution, e.g.  
701 with phosphorus (Daneshgar et al., 2018; Vaccari, 2009), where a pollutant accumulates in soils but  
702 slowly find its way into inland waters through soil erosion. In this respect, it is important to note that it  
703 will be easier to reduce MP inputs to stream networks coming from point sources, e.g. WWTP, whereas  
704 the diffuse input will continue for centuries.

#### 705 *4.6. Targeted application of MP-laden organic fertilizer*

706 The predicted increase in plastics production means that more MP inputs into the environment can be  
707 expected in the future (Borrelle et al., 2020; Horton, 2022). Because of this, it is necessary to consider  
708 what measures can be taken to reduce or avoid the entry of MP into the various environmental  
709 compartments. The results of S2 have shown that the application of organic fertilizer (without TW)  
710 containing MP at a distance of more than 100 m from the stream network can reduce MP entry into  
711 surface waters via soil erosion by up to 46% compared to S1 (Fig. 7). By contrast (unplanned) application  
712 of MP-laden soil amendments in the proximity of the stream network increase MP supply (by 53% in  
713 our scenario).

714 This highlights the potential impact of optimized landscape management taking into account the  
715 location of any agricultural management activity. It also shows that, in addition to soil conservation in  
716 the field to prevent soil erosion, general changes in catchment management affecting hydrological and  
717 sedimentological connectivity have important implications for the transport of sediments and pollutants.  
718 Therefore, the location of soil additives, which are usually used to close production cycles, should be

719 considered for future use. This consideration can have a significant influence on the subsequent erosion  
720 transport and redistribution of, for example, MP within a whole river catchment.

## 721 **5. Conclusion**

722 In this study, the transport of MP eroded from arable land was modelled across a mesoscale landscape.  
723 Sewage sludge, compost, atmospheric deposition and tyre wear were considered as MP sources. Tyre  
724 wear not only represented the largest MP input to arable land. It also generated the largest MP delivery  
725 rates to the stream network, although tyre wear is not widespread on arable land, only occurring on fields  
726 near the roads. In percentage terms, only a small fraction ( $< 0.2\%$ ) of all MP applied to arable land ended  
727 up directly in the stream network via soil erosion. However, the MP mass delivered into the stream  
728 network represented a serious amount of MP input. The modelled MP delivery into the stream network  
729 was in the same range of potential MP inputs from wastewater treatment plants from this rural area.

730 In addition, it was shown that most of the MP applied to arable soils remains in the topsoil (0–20 cm)  
731 for decades. Tillage produces a regular homogenization, and the MP stays available for surface runoff  
732 and water erosion in the long term. Based on a series of scenarios modelled up to 2100 with no more MP  
733 input from 2020 onwards, similar MP delivery rates (compared to 2020) could still be identified. This  
734 implies that arable land represents an MP sink on the one hand and a long-term MP source for inland  
735 waters on the other.

736 Using the soil profile update component included in the SPEROS-MP model, the MP concentrations  
737 along the soil profile could be determined to a depth of 1 m. It was modelled that 5% of the MP applied  
738 to arable land is translocated into the subsoil ( $> 20$  cm) by tillage and water erosion. Located below the  
739 plough horizon, the MP is out of reach for future lateral surface runoff erosion processes. Based on the  
740 spatially distributed erosion model, it was also demonstrated that most of the eroded MP leaving arable

741 land is deposited in grassland (1% of applied MP). Especially in areas of the river valleys, these  
742 accumulations could represent a concentrated MP entry into the stream network in the event of a flood.

743 The most effective protection for arable land would probably be to limit or ban the application of MP-  
744 contaminated organic fertilizers. The following measures would be conceivable to protect water bodies  
745 from MP inputs through soil erosion. Our model scenario showed that the targeted application of MP-  
746 contaminated organic fertilizer at a distance of at least 100 m from the water body led to a significantly  
747 lower MP delivery rate from this MP source. The deliberate creation of grass strips in the landscape to  
748 protect against erosion would also be an option. However, it is important to consider that all calculated  
749 and modelled cases were dominated by tyre wear, which is difficult to manage, especially in regions with  
750 a high population and dense road network. Therefore, in order to preserve soil as a valuable resource, as  
751 well as to protect the terrestrial and aquatic ecosystem from MP pollution and its effects, we should focus  
752 on limiting MP emissions to the environment in general as much as possible.

753



754 **Competing interests**

755 Some authors are members of the editorial board of journal SOIL. The peer-review process  
756 was guided by an independent editor, and the authors have also no other competing interests  
757 to declare.

758 **Acknowledgments**

759 The authors would like to acknowledge the financial support from the Federal Ministry of Education  
760 and Research towards this research as part of the initiative Plastics in the Environment (funding number  
761 02WPL1447A-G). In addition, we would like to thank the Bavarian State Office of Agriculture (LfL)  
762 and the Bavarian State Office for the Environment (LfU) for providing and accessing Bavaria-wide data,  
763 as well as providing the modelling data for the Glonn catchment area. Finally, special thanks go to the  
764 members of the Soil and Water Resources Research Group in Augsburg for supporting this work.

765

766 **References**

767

- 768 Accinelli C, Abbas HK, Bruno V, Vicari A, Little NS, Ebelhar MW, et al. Minimizing abrasion losses from film-  
769 coated corn seeds. *Journal of Crop Improvement* 2021; 35: 666-678.
- 770 Aves AR, Revell LE, Gaw S, Ruffell H, Schuddeboom A, Wotherspoon NE, et al. First evidence of microplastics  
771 in Antarctic snow. *The Cryosphere* 2022; 16: 2127-2145.
- 772 Baensch-Baltruschat B, Kocher B, Kochleus C, Stock F, Reifferscheid G. Tyre and road wear particles-A  
773 calculation of generation, transport and release to water and soil with special regard to German roads.  
774 *Science of The Total Environment* 2020; 752: 141939.
- 775 BAYSIS BS. *Straßenverkehrszählungen (SVZ)*, 2015.
- 776 Bertling J, Zimmermann T, Rödiger L. *Kunststoffe in der Umwelt: Emissionen in landwirtschaftlich genutzte Böden.*  
777 *Fraunhofer UMSICHT* 2021: 220.
- 778 Bläsing M, Amelung W. Plastics in soil: Analytical methods and possible sources. *Science of the Total*  
779 *Environment* 2018; 612: 422-435.
- 780 Borrelle SB, Ringma J, Law KL, Monahan CC, Lebreton L, McGivern A, et al. Predicted growth in plastic waste  
781 exceeds efforts to mitigate plastic pollution. *Science* 2020; 369: 1515-1518.
- 782 Borthakur A, Leonard J, Koutnik VS, Ravi S, Mohanty SK. Inhalation risks of wind-blown dust from biosolid-  
783 applied agricultural lands: Are they enriched with microplastics and PFAS? *Current Opinion in*  
784 *Environmental Science & Health* 2022; 25: 100309.
- 785 Brahney J, Hallerud M, Heim E, Hahnenberger M, Sukumaran S. Plastic rain in protected areas of the United States.  
786 *Science* 2020; 368: 1257-1260.
- 787 Brandes E. *Die Rolle der Landwirtschaft bei der (Mikro-) Plastik-Belastung in Böden und Oberflächengewässern.*  
788 2020.
- 789 Brandes E, Henseler M, Kreins P. Identifying hot-spots for microplastic contamination in agricultural soils—a  
790 spatial modelling approach for Germany. *Environmental Research Letters* 2021; 16: 104041.
- 791 Brandhuber R, Auerswald K, Lang R, Müller A, Treisch M. *ABAG interaktiv, Version 2.0.* Bayerische  
792 *Landesanstalt für Landwirtschaft, Freising.* 2018.
- 793 Braun M, Mail M, Heyse R, Amelung W. Plastic in compost: Prevalence and potential input into agricultural and  
794 horticultural soils. *Science of The Total Environment* 2021; 760: 143335.
- 795 Bullard JE, Ockelford A, O'Brien P, Neuman CM. Preferential transport of microplastics by wind. *Atmospheric*  
796 *Environment* 2021; 245: 118038.
- 797 Cai Y, Wu J, Lu J, Wang J, Zhang C. Fate of microplastics in a coastal wastewater treatment plant: Microfibers  
798 could partially break through the integrated membrane system. *Frontiers of Environmental Science &*  
799 *Engineering* 2022; 16: 1-10.
- 800 Chia RW, Lee J-Y, Kim H, Jang J. Microplastic pollution in soil and groundwater: a review. *Environmental*  
801 *Chemistry Letters* 2021; 19: 4211-4224.
- 802 Colin G, Cooney J, Carlsson D, Wiles D. Deterioration of plastic films under soil burial conditions. *Journal of*  
803 *Applied Polymer Science* 1981; 26: 509-519.
- 804 Corcoran PL. Degradation of microplastics in the environment. *Handbook of Microplastics in the Environment.*  
805 *Springer*, 2022, pp. 531-542.
- 806 Daneshgar S, Callegari A, Capodaglio AG, Vaccari D. The potential phosphorus crisis: resource conservation and  
807 possible escape technologies: a review. *Resources* 2018; 7: 37.
- 808 Desmet P, Govers G. A GIS procedure for automatically calculating the USLE LS factor on topographically  
809 complex landscape units. *Journal of soil and water conservation* 1996; 51: 427-433.
- 810 Dlugoß V, Fiener P, Van Oost K, Schneider K. Model based analysis of lateral and vertical soil carbon fluxes  
811 induced by soil redistribution processes in a small agricultural catchment. *Earth Surface Processes and*  
812 *Landforms* 2012; 37: 193-208.
- 813 DWD DW. *Klimadaten direkt zum Download. 3. Rasterfelder für Deutschland.* 2020.
- 814 Edo C, González-Pleiter M, Leganés F, Fernández-Piñas F, Rosal R. Fate of microplastics in wastewater treatment  
815 plants and their environmental dispersion with effluent and sludge. *Environmental Pollution* 2020; 259:  
816 113837.

817 Eibes PM, Gabel F. Floating microplastic debris in a rural river in Germany: Distribution, types and potential  
818 sources and sinks. *Science of The Total Environment* 2022; 816: 151641.

819 Feuilletoy P, César G, Benguigui L, Grohens Y, Pillin I, Bewa H, et al. Degradation of polyethylene designed for  
820 agricultural purposes. *Journal of Polymers and the Environment* 2005; 13: 349-355.

821 Fiener P, Dlugoš V, Van Oost K. Erosion-induced carbon redistribution, burial and mineralisation - Is the episodic  
822 nature of erosion processes important? *Catena* 2015; 133: 282-292.

823 Fiener P, Dostál T, Krása J, Schmaltz E, Strauss P, Wilken F. Operational USLE-Based Modelling of Soil Erosion  
824 in Czech Republic, Austria, and Bavaria—Differences in Model Adaptation, Parametrization, and Data  
825 Availability. *Applied Sciences* 2020; 10: 3647.

826 Fiener P, Govers G, Van Oost K. Evaluation of a dynamic multi-class sediment transport model in a catchment  
827 under soil-conservation agriculture. *Earth Surface Processes and Landforms* 2008; 33: 1639-1660.

828 Fiener P, Wilken F, Aldana-Jague E, Deumlich D, Gómez J, Guzmán G, et al. Uncertainties in assessing tillage  
829 erosion—how appropriate are our measuring techniques? *Geomorphology* 2018; 304: 214-225.

830 Frias JP, Nash R. Microplastics: Finding a consensus on the definition. *Marine pollution bulletin* 2019; 138: 145-  
831 147.

832 Gehrke I, Dresen B, Blömer J, Sommer H, Lindow F, Röckle R. TyreWearMapping. Digitales Planungs-und  
833 Entscheidungsinstrument zur Verteilung, Ausbreitung und Quantifizierung von Reifenabrieb in  
834 Deutschland. Schlussbericht. 2021.

835 Govers G, Vandaele K, Desmet P, Poesen J, Bunte K. The role of tillage in soil redistribution on hillslopes.  
836 *European Journal of Soil Science* 1994; 45: 469-478.

837 Guo J-J, Huang X-P, Xiang L, Wang Y-Z, Li Y-W, Li H, et al. Source, migration and toxicology of microplastics  
838 in soil. *Environment International* 2020; 137: 105263.

839 Habib RZ, Thiemann T, Al Kendi R. Microplastics and wastewater treatment plants—a review. *Journal of Water  
840 Resource and Protection* 2020; 12: 1.

841 Heinze WM, Mitrano DM, Cornelis G. Bioturbation-driven transport of microplastic fibres in soil. *Copernicus  
842 Meetings*, 2022.

843 Hillenbrand T, Toussaint D, Boehm E, Fuchs S, Scherer U, Rudolphi A, et al. Discharges of copper, zinc and lead  
844 to water and soil. Analysis of the emission pathways and possible emission reduction measures; Eintraege  
845 von Kuper, Zink und Blei in Gewaesser und Boeden. Analyse der Emissionspfade und moeglicher  
846 Emissionsminderungsmassnahmen. 2005.

847 Horton AA. Plastic pollution: When do we know enough? *Journal of Hazardous Materials* 2022; 422: 126885.

848 Huerta Lwanga E, Thapa B, Yang X, Gertsen H, Salanki T, Geissen V, et al. Decay of low-density polyethylene  
849 by bacteria extracted from earthworm's guts: A potential for soil restoration. *Sci Total Environ* 2017; 624:  
850 753-757.

851 Hurley RR, Nizzetto L. Fate and occurrence of micro(nano)plastics in soils: Knowledge gaps and possible risks.  
852 *Current Opinion in Environmental Science & Health* 2018; 1: 6-11.

853 Keller B, Centeri C, Szabó JA, Szalai Z, Jakab G. Comparison of the applicability of different soil erosion models  
854 to predict soil erodibility factor and event soil losses on loess slopes in Hungary. *Water* 2021; 13: 3517.

855 Kim Y-N, Yoon J-H, Kim K-HJ. Microplastic contamination in soil environment—a review. *Soil Science Annual  
856 2021*; 71: 300-308.

857 Klein M, Fischer EK. Microplastic abundance in atmospheric deposition within the Metropolitan area of Hamburg,  
858 Germany. *Science of the Total Environment* 2019; 685: 96-103.

859 Knight LJ, Parker-Jurd FN, Al-Sid-Cheikh M, Thompson RC. Tyre wear particles: an abundant yet widely  
860 unreported microplastic? *Environmental Science and Pollution Research* 2020a; 1-10.

861 Knight LJ, Parker-Jurd FN, Al-Sid-Cheikh M, Thompson RC. Tyre wear particles: an abundant yet widely  
862 unreported microplastic? *Environmental Science and Pollution Research* 2020b; 27: 18345-18354.

863 Kocher B, Brose S, Feix J, Görg C, Peters A, Schenker K. Stoffeinträge in den Straßenseitenraum-Reifenabrieb.  
864 BERICHTE DER BUNDESANSTALT FUER STRASSENWESEN. UNTERREIHE  
865 VERKEHRSTECHNIK 2010.

866 Krasa J, Dostal T, Van Rompaey A, Vaska J, Vrana K. Reservoirs' siltation measurements and sediment transport  
867 assessment in the Czech Republic, the Vrchlice catchment study. *Catena* 2005; 64: 348-362.

868 LfL BLfL. Erosionsatlas Bayern. 2023.

869 LfStaD BLfSuD. Statistisches Jahrbuch für Bayern. 2022.

870 LfU BLfU. Abfallwirtschaft–Hausmüll in Bayern–Bilanzen 2002. Bayerisches Landesamt für Umweltschutz,  
871 Augsburg 1990-2020.

872 Li H, Lu X, Wang S, Zheng B, Xu Y. Vertical migration of microplastics along soil profile under different crop  
873 root systems. *Environmental Pollution* 2021; 278: 116833.

874 Li S, Ding F, Flury M, Wang Z, Xu L, Li S, et al. Macro-and microplastic accumulation in soil after 32 years of  
875 plastic film mulching. *Environmental Pollution* 2022; 300: 118945.

876 Lian J, Liu W, Meng L, Wu J, Zeb A, Cheng L, et al. Effects of microplastics derived from polymer-coated fertilizer  
877 on maize growth, rhizosphere, and soil properties. *Journal of Cleaner Production* 2021; 318: 128571.

878 Liu EK, He WQ, Yan CR. ‘White revolution’ to ‘white pollution’—agricultural plastic film mulch in China.  
879 *Environmental Research Letters* 2014; 9.

880 Lwanga EH, Beriot N, Corradini F, Silva V, Yang X, Baartman J, et al. Review of microplastic sources, transport  
881 pathways and correlations with other soil stressors: a journey from agricultural sites into the environment.  
882 *Chemical and Biological Technologies in Agriculture* 2022; 9: 1-20.

883 Meinen BU, Robinson DT. Agricultural erosion modelling: Evaluating USLE and WEPP field-scale erosion  
884 estimates using UAV time-series data. *Environmental Modelling & Software* 2021; 137: 104962.

885 Mennekes D, Nowack B. Tire wear particle emissions: Measurement data where are you? *Science of The Total*  
886 *Environment* 2022; 830: 154655.

887 Mintenig S, Int-Veen I, Löder M, Gerdt G. Mikroplastik in ausgewählten Kläranlagen des Oldenburgisch-  
888 Ostfriesischen Wasserverbandes (OOWV) in Niedersachsen. 2014.

889 Motto HL, Daines RH, Chilko DM, Motto CK. Lead in soils and plants: its relation to traffic volume and proximity  
890 to highways. *Environmental Science & Technology* 1970; 4: 231-237.

891 Müller A, Kocher B, Altmann K, Braun U. Determination of tire wear markers in soil samples and their distribution  
892 in a roadside soil. *Chemosphere* 2022; 294: 133653.

893 Murphy F, Ewins C, Carbonnier F, Quinn B. Wastewater Treatment Works (WwTW) as a Source of Microplastics  
894 in the Aquatic Environment. *Environ Sci Technol* 2016; 50: 5800-8.

895 Nadeu E, Gobin A, Fiener P, Van Wesemael B, Van Oost K. Modelling the impact of agricultural management on  
896 soil carbon stocks at the regional scale: the role of lateral fluxes. *Global Change Biology* 2015: DOI:  
897 10.1111/gcb.12889.

898 Nasseri S, Azizi N. Occurrence and Fate of Microplastics in Freshwater Resources. *Microplastic Pollution*.  
899 Springer, 2022, pp. 187-200.

900 Ng E-L, Lwanga EH, Eldridge SM, Johnston P, Hu H-W, Geissen V, et al. An overview of microplastic and  
901 nanoplastic pollution in agroecosystems. *Science of the total environment* 2020; 627: 1377-1388.

902 Ng EL, Lwanga EH, Eldridge SM, Johnston P, Hu HW, Geissen V, et al. An overview of microplastic and  
903 nanoplastic pollution in agroecosystems. *Science of the Total Environment* 2018; 627: 1377-1388.

904 Nunes JP, Wainwright J, Biolders CL, Darboux F, Fiener P, Finger D, et al. Better models are more effectively  
905 connected models. *Earth Surface Processes and Landforms* 2018; 43.

906 Pérez-Reverón R, González-Sálamo J, Hernández-Sánchez C, González-Pleiter M, Hernández-Borges J, Díaz-Peña  
907 FJ. Recycled wastewater as a potential source of microplastics in irrigated soils from an arid-insular  
908 territory (Fuerteventura, Spain). *Science of The Total Environment* 2022; 817: 152830.

909 Rehm R, Zeyer T, Schmidt A, Fiener P. Soil erosion as transport pathway of microplastic from agriculture soils to  
910 aquatic ecosystems. *Science of The Total Environment* 2021; 795: 148774.

911 Rillig MC, Ziersch L, Hempel S. Microplastic transport in soil by earthworms. *Sci Rep* 2017; 7: 1362.

912 Sajjad M, Huang Q, Khan S, Khan MA, Yin L, Wang J, et al. Microplastics in the soil environment: A critical  
913 review. *Environmental Technology & Innovation* 2022: 102408.

914 Schell T, Hurley R, Buenaventura NT, Mauri PV, Nizzetto L, Rico A, et al. Fate of microplastics in agricultural  
915 soils amended with sewage sludge: Is surface water runoff a relevant environmental pathway?  
916 *Environmental Pollution* 2022; 293: 118520.

917 Scheurer M, Bigalke M. Microplastics in Swiss Floodplain Soils. *Environmental science & technology* 2018.

918 Schleyen P. Abwasserbehandlung (nach 1945). *Historisches Lexikon Bayerns* 2017.

919 Schmidt J, v.Werner M, Michael A. Application of the EROSION 3D model to the CATSOP watershed, The  
920 Netherlands. *Catena* 1999; 37: 449-456.

921 Schwertmann U, Vogl W, Kainz M. *Bodenerosion durch Wasser*. Ulmer Verlag, 64 p 1987.

922 Singh S, Bhagwat A. Microplastics: A potential threat to groundwater resources. *Groundwater for Sustainable*

923 *Development* 2022; 100852.

924 Sommer F, Dietze V, Baum A, Sauer J, Gilge S, Maschowski C, et al. Tire abrasion as a major source of

925 microplastics in the environment. *Aerosol and Air Quality Research* 2018; 18: 2014-2028.

926 StMB. *Verkehrsentwicklung*. 2023.

927 Tang KHD, Hadibarata T. Microplastics removal through water treatment plants: Its feasibility, efficiency, future

928 prospects and enhancement by proper waste management. *Environmental Challenges* 2021; 5: 100264.

929 Tian L, Jinjin C, Ji R, Ma Y, Yu X. Microplastics in agricultural soils: sources, effects, and their fate. *Current*

930 *Opinion in Environmental Science & Health* 2022; 25: 100311.

931 Unice KM, Weeber MP, Abramson MM, Reid RCD, van Gils JAG, Markus AA, et al. Characterizing export of

932 land-based microplastics to the estuary - Part I: Application of integrated geospatial microplastic transport

933 models to assess tire and road wear particles in the Seine watershed. *Science of the Total Environment*

934 2019; 646: 1639-1649.

935 Vaccari DA. Phosphorus: a looming crisis. *Scientific American* 2009; 300: 54-59.

936 Van Oost K, Govers G, De Alba S, Quine T. Tillage erosion: a review of controlling factors and implications for

937 soil quality. *Progress in Physical Geography* 2006; 30: 443-466.

938 Van Oost K, Govers G, Desmet P. Evaluating the effects of changes in landscape structure on soil erosion by water

939 and tillage. *Landscape ecology* 2000; 15: 577-589.

940 Van Oost K, Govers G, Quine TA, Heckrath G, Olesen JE, De Gryze S, et al. Landscape-scale modeling of carbon

941 cycling under the impact of soil redistribution: The role of tillage erosion. *Global Biogeochemical Cycles*

942 2005a; 19.

943 Van Oost K, Govers G, Van Muysen W. A process-based conversion model for caesium-137 derived erosion rates

944 on agricultural land: An integrated spatial approach. *Earth Surface Processes and Landforms: The Journal*

945 *of the British Geomorphological Research Group* 2003; 28: 187-207.

946 Van Oost K, Quine T, Govers G, Heckrath G. Modeling soil erosion induced carbon fluxes between soil and

947 atmosphere on agricultural land using SPEROS-C. In: Roose EJ, Lal R, Feller C, Barthes B, Stewart BA,

948 editors. *Advances in soil science. Soil erosion and carbon dynamics*. CRC Press, Boca Raton, 2005b, pp.

949 37-51.

950 Van Rompaey AJ, Verstraeten G, Van Oost K, Govers G, Poesen J. Modelling mean annual sediment yield using

951 a distributed approach. *Earth Surface Processes and Landforms* 2001; 26: 1221-1236.

952 Verstraeten G, Prosser IP. Modelling the impact of land-use change and farm dam construction on hillslope

953 sediment delivery to rivers at the regional scale. *Geomorphology* 2008; 98: 199-212.

954 Viaroli S, Lancia M, Re V. Microplastics contamination of groundwater: Current evidence and future perspectives.

955 A review. *Science of The Total Environment* 2022: 153851.

956 Wagner S, Hüffer T, Klöckner P, Wehrhahn M, Hofmann T, Reemtsma T. Tire wear particles in the aquatic

957 environment-a review on generation, analysis, occurrence, fate and effects. *Water research* 2018; 139: 83-

958 100.

959 Waldschläger K, Schüttrumpf H. Infiltration Behavior of Microplastic Particles with Different Densities, Sizes,

960 and Shapes—From Glass Spheres to Natural Sediments. *Environmental Science & Technology* 2020; 54:

961 9366-9373.

962 Weber CJ, Santowski A, Chiffard P. Investigating the dispersal of macro-and microplastics on agricultural fields

963 30 years after sewage sludge application. *Scientific reports* 2022; 12: 1-13.

964 Weithmann N, Möller JN, Löder MG, Piehl S, Laforsch C, Freitag R. Organic fertilizer as a vehicle for the entry

965 of microplastic into the environment. *Science Advances* 2018; 4: eaap8060.

966 Werkenthin M, Kluge B, Wessolek G. Metals in European roadside soils and soil solution—A review.

967 *Environmental Pollution* 2014; 189: 98-110.

968 Wheeler G, Rolfe G. The relationship between daily traffic volume and the distribution of lead in roadside soil and

969 vegetation. *Environmental Pollution* (1970) 1979; 18: 265-274.

970 Wik A, Dave G. Occurrence and effects of tire wear particles in the environment—A critical review and an initial

971 risk assessment. *Environmental pollution* 2009; 157: 1-11.

972 Witzig C, Wörle K, Földi C, Rehm R, Reuwer A-K, Ellerbrake K, et al. Mikroplastik in Binnengewässern.  
973 Untersuchung und Modellierung des Eintrags und Verbleibs im Donaugebiet als Grundlage für  
974 Maßnahmenplanung. MICBIN Abschlussbericht. 2021.

975 WRB IWG. World reference base for soil resources 2014, update 2015. International soil classification system for  
976 naming soils and creating legends for soil maps. World Soil Resources Reports No. 106. FAO 2015.

977 Wright S, Ulke J, Font A, Chan K, Kelly F. Atmospheric microplastic deposition in an urban environment and an  
978 evaluation of transport. *Environment International* 2019; 105411.

979 Zhang L, Xie Y, Liu J, Zhong S, Qian Y, Gao P. An overlooked entry pathway of microplastics into agricultural  
980 soils from application of sludge-based fertilizers. *Environmental science & technology* 2020; 54: 4248-  
981 4255.

982 Zhang Y, Gao T, Kang S, Shi H, Mai L, Allen D, et al. Current status and future perspectives of microplastic  
983 pollution in typical cryospheric regions. *Earth-Science Reviews* 2022; 226: 103924.

984 Zhao S, Zhang Z, Chen L, Cui Q, Cui Y, Song D, et al. Review on migration, transformation and ecological impacts  
985 of microplastics in soil. *Applied Soil Ecology* 2022; 176: 104486.

986 Zhou Y, Wang J, Zou M, Jia Z, Zhou S. Microplastics in soils: A review of methods, occurrence, fate, transport,  
987 ecological and environmental risks. *Science of The Total Environment* 2020: 141368.

988 Zubris KA, Richards BK. Synthetic fibers as an indicator of land application of sludge. *Environ Pollut* 2005; 138:  
989 201-11.

990